AD-A127 615 THE RELATIONSHIP BETWEEN LOW-LEVEL CONVERGENCE AND CONVECTIVE PRECIPITATI.. (U) ILLINOIS STATE WATER SURVEY DIV URBANA A I WATSON ET AL. APR 82 TR-7 1/1

UNCLASSIFIED ARO-15529.9-GS NSF-ATM78-08865 F/G 4/2 NL

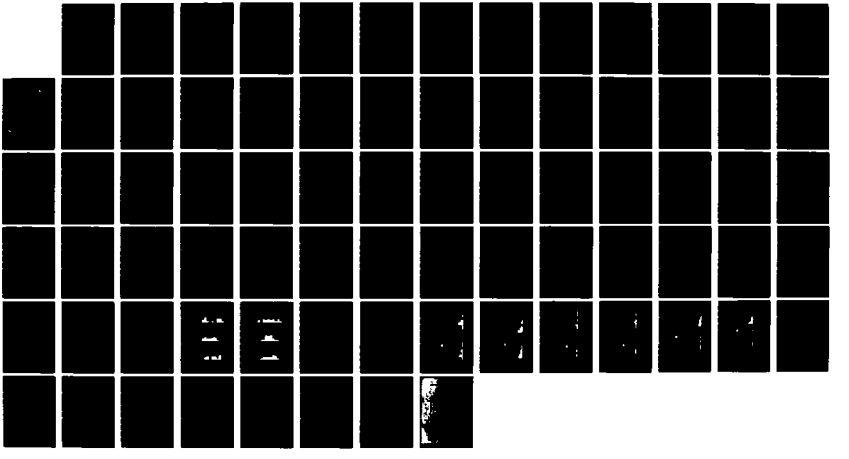

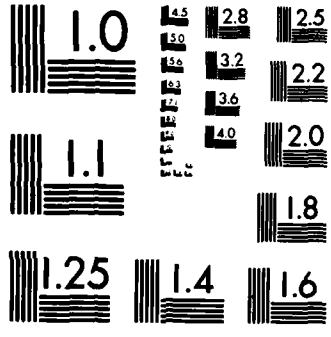

Unclassified

SECURITY CLASSIFICATION OF THIS PAGE (When Data Entered)

REPORT DOCUMENTATION PAGE

READ INSTRUCTIONS BEFORE COMPLETING FORM

1. REPORT NUMBER: 15529.9-GS	2. GOVT ACCESSION NO.
3. RECIPIENT'S CATALOG NUMBER	
4. TITLE (and Subtitle): The Relationship Between Low-Level Convergence and Convective Precipitation in Illinois and South Florida	5. TYPE OF REPORT & PERIOD COVERED: Technical
6. PERFORMING ORG. REPORT NUMBER	
7. AUTHOR(s): Andrew I. Watson, Ronald L. Holle	8. CONTRACT OR GRANT NUMBER(s): ARO MIPR 21-78
9. PERFORMING ORGANIZATION NAME AND ADDRESS: University of Illinois, Champaign, IL 61820	10. PROGRAM ELEMENT, PROJECT, TASK AREA & WORK UNIT NUMBERS
11. CONTROLLING OFFICE NAME AND ADDRESS: U. S. Army Research Office, Post Office Box 12211, Research Triangle Park, NC 27709	12. REPORT DATE: Apr 82 13. NUMBER OF PAGES: 71
14. MONITORING AGENCY NAME & ADDRESS (if different from Controlling Office)	15. SECURITY CLASS. (of this report): Unclassified 15a. DECLASSIFICATION/DOWNGRADING SCHEDULE

16. DISTRIBUTION STATEMENT (of this Report)

Approved for public release; distribution unlimited.

17. DISTRIBUTION STATEMENT (of the abstract entered in Block 20, if different from Report)

18. SUPPLEMENTARY NOTES

The view, opinions, and/or findings contained in this report are those of the author(s) and should not be construed as an official Department of the Army position, policy, or decision, unless so designated by other documentation

19. KEY WORDS (Continue on reverse side if necessary and identify by block number)

precipitation (meteorology)
convection
rainfall

20. ABSTRACT (Continue on reverse side if necessary and identify by block number)

The relationship between total area divergence and convective rainfall was ~~examined using~~ examined using surface data collected during the VIN 1979 field experiment in Illinois. The mesonetwork covered an area of 2800 km^2. Total area divergence, an area-averaged quantity, can also be expressed by the line integral of the normal component of the wind around the network boundary. Total area divergence was statistically related to area rainfall based upon the criterion that a convergence event occurred anytime there was a sustained change in total area

DD FORM 1 JAN 73 1473 EDITION OF 1 NOV 65 IS OBSOLETE

UNCLASSIFIED

SECURITY CLASSIFICATION OF THIS PAGE (When Data Entered)

Abstract cont. — 1/4 ... 5

divergence of less than -25×10^{-6} s^{-1} for greater than 10 minutes. The difference between initial convergence and maximum convergence was related to total area precipitation associated with the convergence. During the 33-day study, there were 106 convergence events. Forty-four of the events had rainfall, and the average was 1.53 mm per event. The correlation coefficient was -0.50. Other meteorological factors also have an influence on convergence and the production of precipitation such as middle-level moisture, stability, and low-level wind speed which improve the statistical relationships in many instances. Weighted convergence, a subset of total area divergence, was also used to develop regression relationships. Weighted convergence is dependent on an inner grid of wind stations. Weighted convergence appeared to filter out weak convergence events, therefore eliminating many no-rain or false alarm convergence events as well as the weaker, unimportant convergence-rainfall periods. When compared with south Florida relationships from an earlier investigation, the Illinois results show that the correlation between convergence and rainfall has dropped a tenth in almost all cases.

State Water Survey Division
METEOROLOGY SECTION
AT THE
UNIVERSITY OF ILLINOIS

Illinois Institute of Natural Resources

THE RELATIONSHIP BETWEEN LOW-LEVEL CONVERGENCE AND CONVECTIVE PRECIPITATION IN ILLINOIS AND SOUTH FLORIDA

Andrew I. Watson
Ronald L. Holle

Office of Weather Research and Modification
Environmental Research Laboratories
National Oceanic and Atmospheric Administration

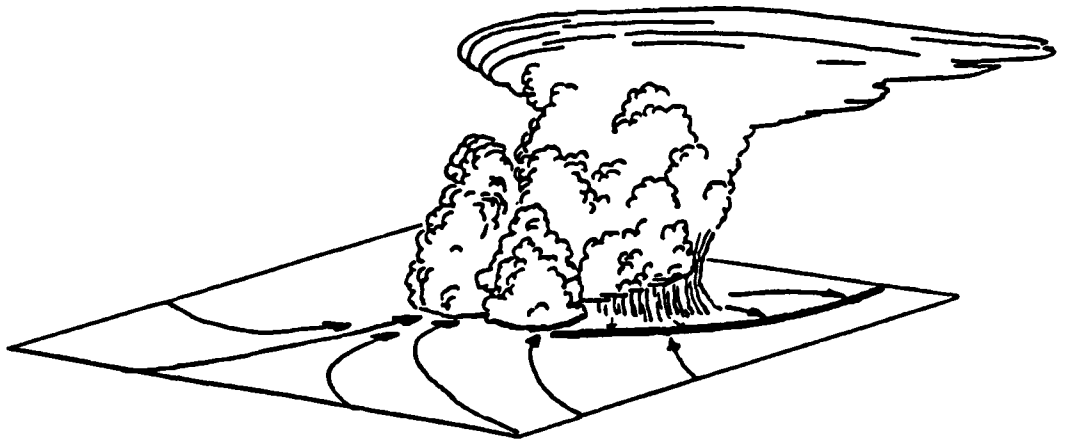

Technical Report 7
NSF Grant ATM 78-08865
Low-Level Convergence and the
Prediction of Convective Precipitation
April 1982

Champaign IL 61820

The project "Low-level Convergence and the Prediction of Convective Precipitation" is a coordinated research effort by the State Water Survey Division of the Illinois Institute of Natural Resources, the Office of Weather Research and Modification in the National Oceanic and Atmospheric Administration, and the Department of Environmental Sciences of the University of Virginia. Support of this research has been provided to the State Water Survey by the Atmospheric Research Section, National Science Foundation, through grant ATM-78-08865. This award includes funds from the Army Research Office and the Air Force Office of Scientific Research of the Department of Defense.

THE RELATIONSHIP BETWEEN LOW-LEVEL CONVERGENCE AND CONVECTIVE PRECIPITATION IN ILLINOIS AND SOUTH FLORIDA

Andrew I. Watson

Ronald L. Holle

Office of Weather Research and Modification
Environmental Research Laboratories, NOAA
Boulder, Colorado 80303

Technical Report 7
NSF Grant ATM 78-08865
Low-Level Convergence and the
Prediction of Convective Precipitation
April 1982

THE RELATIONSHIP BETWEEN LOW-LEVEL CONVERGENCE
AND CONVECTIVE PRECIPITATION IN ILLINOIS AND SOUTH FLORIDA

ABSTRACT

The relationship between total area divergence and convective rainfall was examined using surface data collected during the VIN 1979 field experiment in Illinois. The mesonetwork covered an area of 2800 km^2. Total area divergence, an area-averaged quantity, can also be expressed by the line integral of the normal component of the wind around the network boundary. Total area divergence was statistically related to area rainfall based upon the criterion that a convergence event occurred anytime there was a sustained change in total area divergence of less than -25×10^{-6} s^{-1} for greater than 10 minutes. The difference between initial convergence and maximum convergence was related to total area precipitation associated with the convergence. During the 33-day study, there were 106 convergence events. Forty-four of the events had rainfall, and the average was 1.53 mm per event. The correlation coefficient was -0.50. Other meteorological factors also have an influence on convergence and the production of precipitation such as middle-level moisture, stability, and low-level wind speed which improve the statistical relationships in many instances.

Weighted convergence, a subset of total area divergence, was also used to develop regression relationships. Weighted convergence is dependent on an inner grid of wind stations. Weighted convergence appeared to filter out weak convergence events, therefore eliminating many no-rain or false alarm convergence events as well as the weaker, unimportant convergence-rainfall periods.

When compared with south Florida relationships from an earlier investigation, the Illinois results show that the correlation between convergence and rainfall has dropped a tenth in almost all cases.

Difficulties arise in both regions with this technique. Small convergence events may produce either heavy or light precipitation. In south Florida, the larger convergence events always produced moderate to heavy rain. In Illinois, this was usually the case but several times this pattern was altered by dry outflows accompanied by large convergence originating from convective systems 100 to 200 km from the VIN network. In south Florida, the systems were mainly slow-movers, building and dissipating within the confines of the mesonetwork. In Illinois, the systems were predominantly mature entities, moving rapidly across the network.

The representativeness of surface divergence to boundary-layer divergence was investigated using a 750 km^2 pibal triangle within the VIN network. The correlation of boundary-layer divergence to surface divergence was found to be marginal. Under disturbed meteorological conditions, persistent organization aloft was found and the use of boundary-layer divergence alone as a indicator of convective precipitation is explored.

1. Introduction

This report is the last in a series presenting NOAA's results for work performed under a grant awarded by the National Science Foundation and the Department of Defense to the University of Virginia (UVa), the Illinois State Water Survey (ISWS), and the National Oceanic and Atmospheric Administration (NOAA). This report focuses mainly on the Illinois environment and draws comparisons with the results found in south Florida.

The main objective and emphasis of NOAA has been to investigate a relationship between convergence and rainfall on an area-wide basis with a large set of data. Watson et al. (1981) introduced a method for nowcasting convective precipitation using the surface convergence field in south Florida. The maximum change in total area divergence with time was statistically related to total area rainfall as derived by radar in a region of about 1400 km^2. It was also established that other meteorological factors, such as winds and moisture, play important roles that affect changes in the amounts of convective rainfall. It was found that for slow-moving convective systems, the amount of rainfall per event was 3 times greater than for fast-moving systems and convergence increased 30%. When middle-level moisture (850-500 mb) was large, 2 1/2 times more precipitation was recorded for approximately the same amount of convergence than occurred during dry events. Correlation coeffients between convergence and rainfall were about .5 to .8.

For the Illinois area, the same analysis and statistical techniques will be used to test the convergence-rainfall relationships. A thorough comparison will be made with the south Florida results.

It has been found that in some cases the surface total area divergence time profile yielded little information concerning the production of

precipitation. Therefore, the representativeness of the surface divergence field to boundary-layer divergence is also examined in Illinois. Time-height profiles of divergence are presented under several types of boundary-layer structures.

2. Mesonetwork Data - Collection and Analysis Methods.

a. VIN 1979

The VIN (UVa, ISWS, NOAA) surface network was designed to study the relationship between surface wind convergence and convective rainfall. The network was located in a 2800-km^2 region near Champaign, Illinois, in east-central Illinois. It was a two-month effort beginning 27 June 1979. The principle (or inner) network (Fig. 1) included a rectangular grid of 49 sites, 6.4 km apart. Twenty-seven of these sites were a part of the NCAR PAM (Portable Automated Mesonet) network (Brock and Govind, 1977). Meteorological quantities such as pressure, temperature, moisture, rainfall, and winds were recorded in 1-min increments at these stations. The remainder of the sites in the inner network had only analog wind-recording devices. An outer ring of 17 analog stations surrounded the inner network on three sides by 9.6 km (see Fig. 1). Winds, temperature, relative humidity, and pressure were recorded at most of these sites. A dense, rectangular grid of 260 rain gages, 4.8 km apart, covered the entire surface network.

Supplementary measurements were made at three pibal sites located at the northwest and southwest corners and on the eastern border of the inner network (Fig. 1); time-lapse cameras were situated at the two westernmost pibal sites. Radiosonde thermodynamic data were collected at the Champaign airport. Additional rawinsonde data were recorded at the National Weather

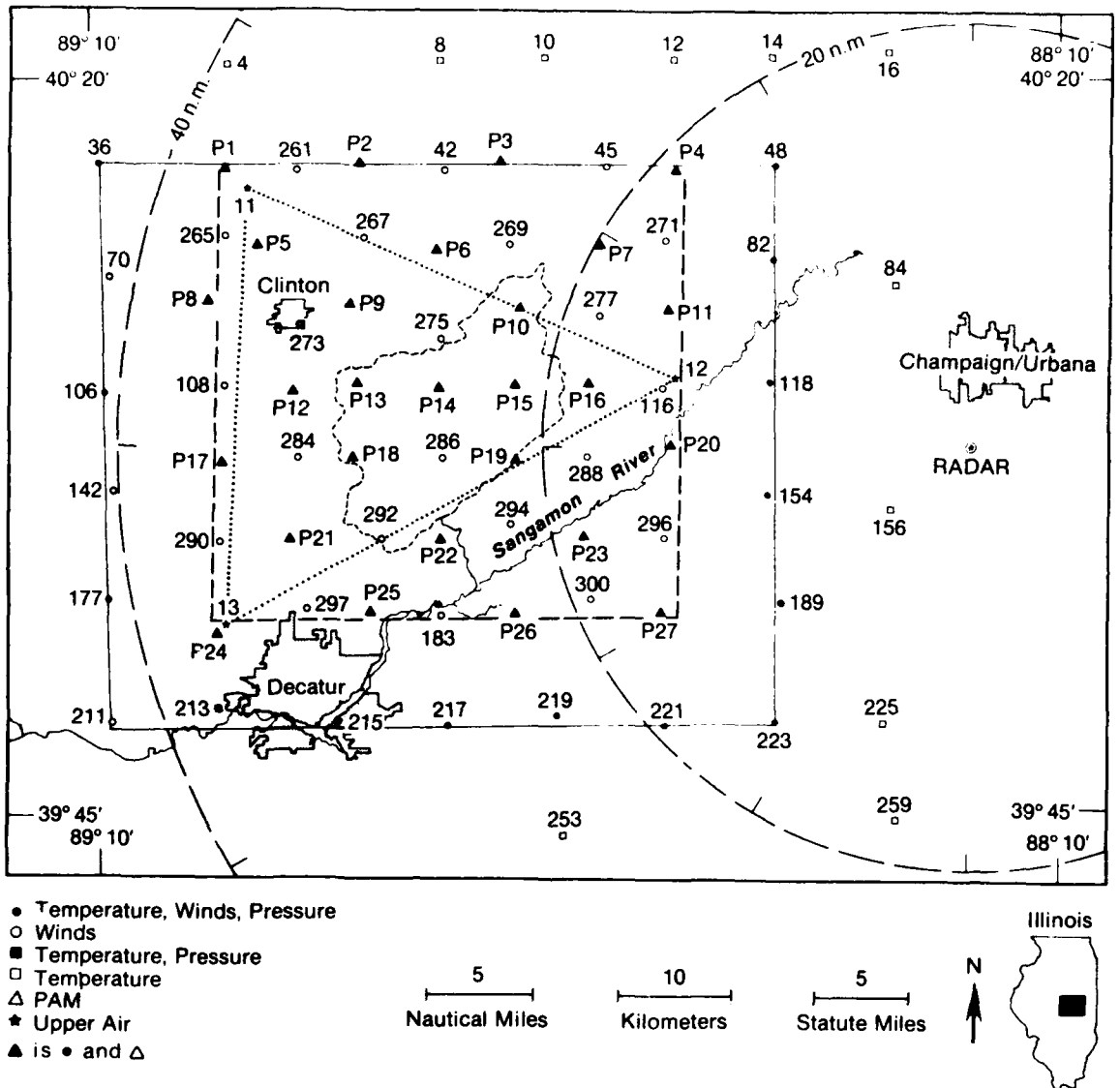

Figure 1. VIN 1979 mesonetwork. The dashed line encloses the inner wind network, the solid line shows the outer network boundary, and the dotted line shows the triangular pibal area.

Service (NWS) stations located at Peoria (about 110 km northwest of VIN network) and Salem, Illinois (about 155 km south).

The ISWS CHILL radar was located at the airport south of Champaign (Fig. 1). The CHILL radar has a dual-wavelength capability: a 10-cm Doppler radar and a 3-cm incoherent radar mounted on the same pedestal. Additional radar capabilities included the NWS WSR-57 surveillance radar located at Marseilles, Illinois (150 km north), and, to a somewhat limited extent, the ISWS HOT radar located at Joliet, Illinois (175 km north).

Intensive-study periods were scheduled on days when deep convection was forecast to take place. Thirty-six such days were chosen during VIN. Special rawinsonde observations were taken at the NWS Peoria and Salem sites at 1300 CDT. Radiosonde soundings at the Champaign site were launched at 1300 and 1800 CDT, and pibal observations at the three inner network locations were taken at 30-min intervals when possible.

For this report, 33 days were identified for processing. Not all of these days were intensive-study days. Selection was based on meteorological conditions, availability of data, and overlapping objectives with the other agencies. Since there was an abundant amount of analog data, many of the days had to agree with case study days identified by the other agencies so that the data reduction effort would be minimized. It was not the objective to have all prefrontal or disturbed days with an abundance of thunderstorm activity. The sample had to contain varying meteorological conditions, including no-rain days, to test the convergence-rainfall relationships. Finally, some days could not be used because of instrumentation outages.

Because of the extensive data reduction effort, only data from the 27 PAM sites of the inner network and 15 outer network stations were combined to provide the information necessary for this study. Fig. 2 provides information

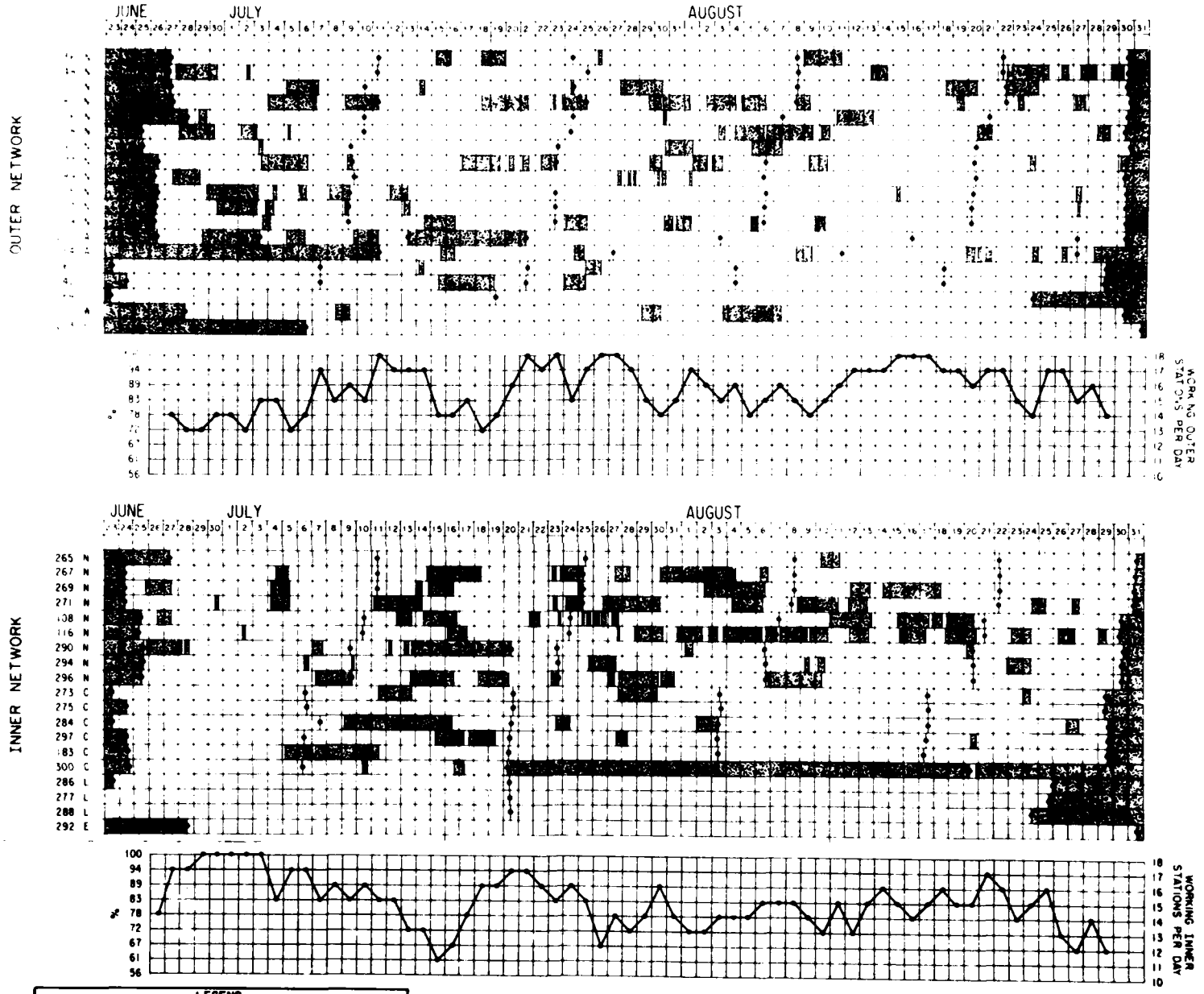

Figure 2. Data summary for analog wind sites for VIN 1979. Shaded areas denote missing data.

on the type of system located at each analog station in both the inner and outer network (Fig. 1). A record of missing data is also provided in Fig. 2.

The surface divergence fields are calculated from 5-min averaged PAM and outer network analog data. A 9x11 grid of equally spaced (6.4 km) points is superimposed upon the original network. Through the use of an objective analysis scheme (Cressman, 1959), the mesonetwork wind data are transformed into a uniform grid of u- and v-components. The values of the wind components at each grid point are then used to compute the divergence quantities.

Rainfall data have been analyzed for each rain gage in the VIN mesonetwork in 5-min increments by the Illinois State Water Survey. Rainfall data to be presented are an area depth that has accumulated in 5 min across the VIN mesonetwork.

Pibal winds are determined by conventional methods using published NWS rise rates. Divergence aloft is calculated at each level (MSL) by determining the area defined by the location of the three balloons at that height. A new area is calculated using the wind speeds at that level. Finally, divergence becomes the fractional rate of change of the two horizontal areas. A more comprehensive description of the VIN 1979 field program can be found in Ackerman et al. (1982).

b. FACE 1975

The FACE (Florida Area Cumulus Experiment) 1975 project was a 2-month effort that was conducted in a 1400-km^2 area just south of Lake Okeechobee in south Florida beginning 1 July 1975. The network consisted of 46 analog surface wind recorders in a 32 by 45-km region with one station every 6.4 km. A smaller rain-gage network (598 km^2) with one station every 3.2 km provided ground truth for daily radar-to-rain gage comparison. Rainfall was derived from radar rather than rain gages because the areal coverage of the

rain-gage network was considerably less than the areal coverage of the wind network. Radar data were obtained from the WSR-57 employed by the National Hurricane Center. The returned power from a scan every 5 min was digitized and a gage-to-radar rainfall ratio (G/R) was used to adjust the radar values. Analysis of the wind data was handled exactly as it was for VIN. A more detailed description of FACE 1975 data collection and analysis methods is given in Watson et al. (1981).

3. Illinois Divergence-Rainfall Relationships

a. Area-Averaged Divergence

The Thunderstorm Project found that deep convection was caused by convergence in the middle and lower troposphere (Byers and Braham, 1949). Ulanski and Garstang (1978) suggested that it may be possible to nowcast the onset and intensity of convective precipitation through the use of surface convergence. Watson et al. (1981) and Watson and Blanchard (1982) examined area-averaged divergence and its possibility as a short-term forecasting tool using south Florida data. The study here extends the techniques developed in south Florida to a more complicated environment of the Midwest United States.

Several types of area-averaged divergence are important for this study:

(1) Total Area Divergence

The average of all divergence values in the rectangular mesoscale grid as derived from the objective analysis scheme for each 5-min period. This is the same as the line integral around the boundary.

(2) Weighted Convergence (Divergence)

The summation of only convergence (divergence) values at grid points divided by the total number of grid points for each 5-min period.

Figs. 3 - 6 provide examples of total area divergence, weighted convergence and divergence, and associated area rainfall. The classic sinusoidal pattern of total area divergence coupled with precipitation is clearly reflected for 13 July (Fig. 3) and 14 July (Fig. 4). As shown by Cooper et al. (1982) and Watson et al. (1981), there is a direct relationship between the strength of the sinusoidal pattern and the production of precipitation. Weighted convergence and weighted divergence each exhibit one peak associated with inflow and outflow. When weighted convergence is subtracted from weighted divergence, the resultant is total area divergence. Fig. 5 for 27 July 1979 shows that the divergence pattern is not always straightforward. The inflow pattern for the rain event beginning at 1300 CDT is missing. Examination of weighted convergence reveals very weak convergence between 1100 and 1500 CDT. There is no clue in the surface convergence pattern that a significant rain event will happen. Finally, an example of a no-rain day is given by 25 August 1979 (Fig. 6). All of the convergence and divergence patterns are very flat and have no significant perturbations. The VIN field program summary (Ackerman et al. 1982) contains the time profiles of total area divergence and area precipitation for the 33 analysis days.

b. A Convergence Event

It was found by Watson et al. (1981) that the most important contributing factor concerning area divergence when related to rainfall is the maximum change in total area divergence, i.e. the difference in total area divergence

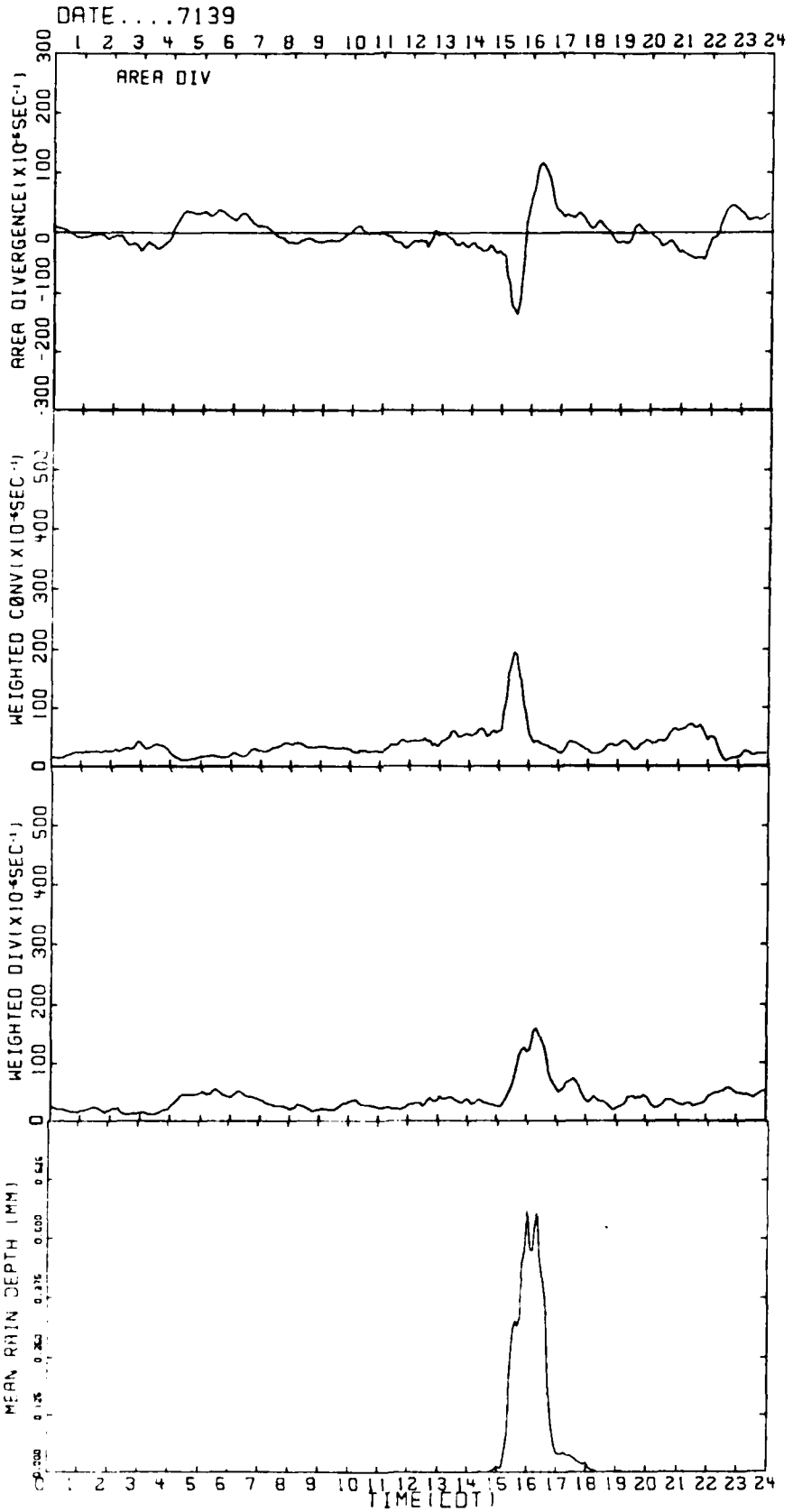

Figure 3. Time profiles of total area divergence, weighted convergence, weighted divergence, and area rain depth for 13 July 1979.

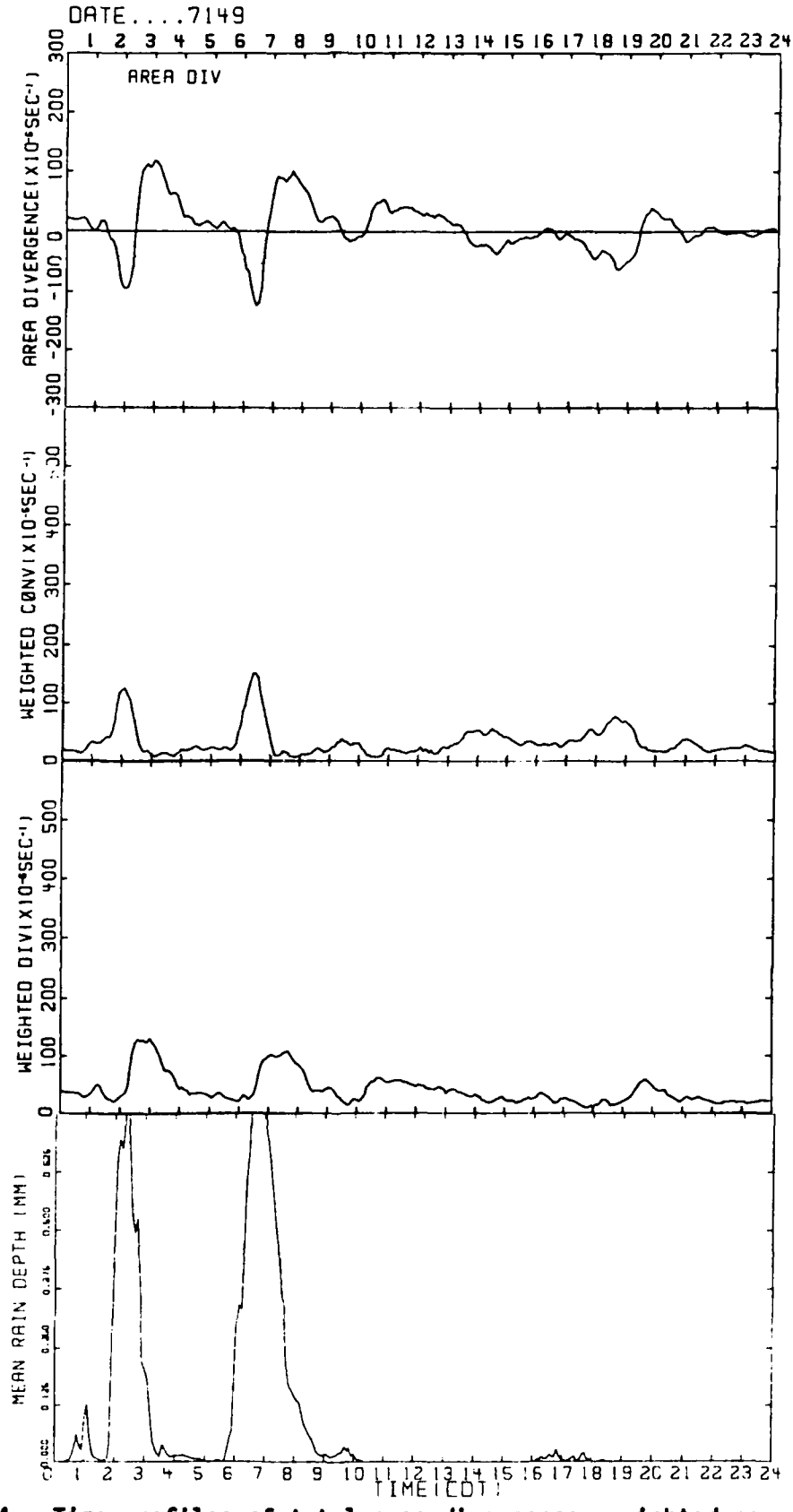

Figure 4. Time profiles of total area divergence, weighted convergence, weighted divergence, and area rain depth for 14 July 1979.

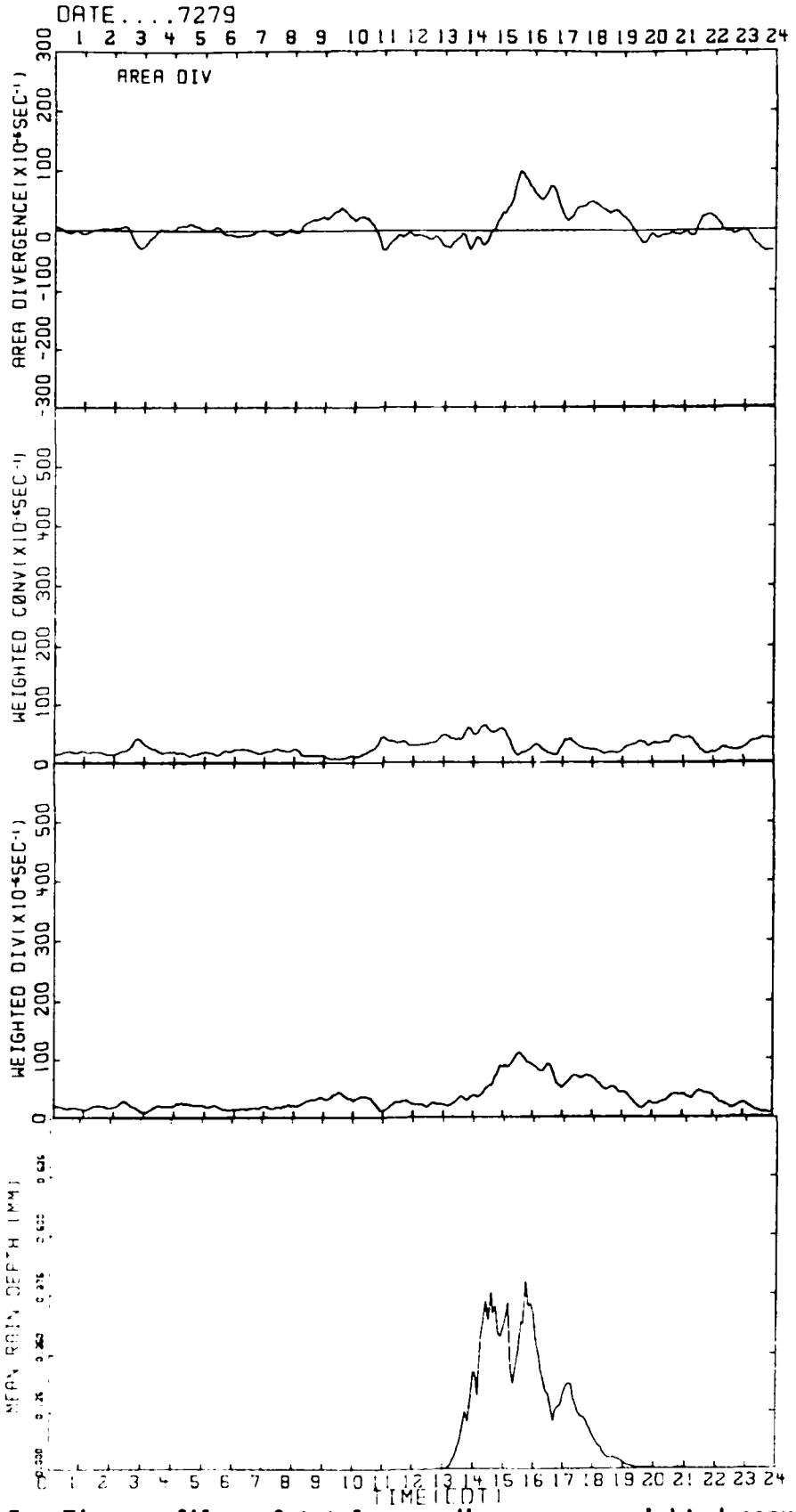

Figure 5. Time profiles of total area divergence, weighted convergence, weighted divergence, and area rain depth for 27 July 1979.

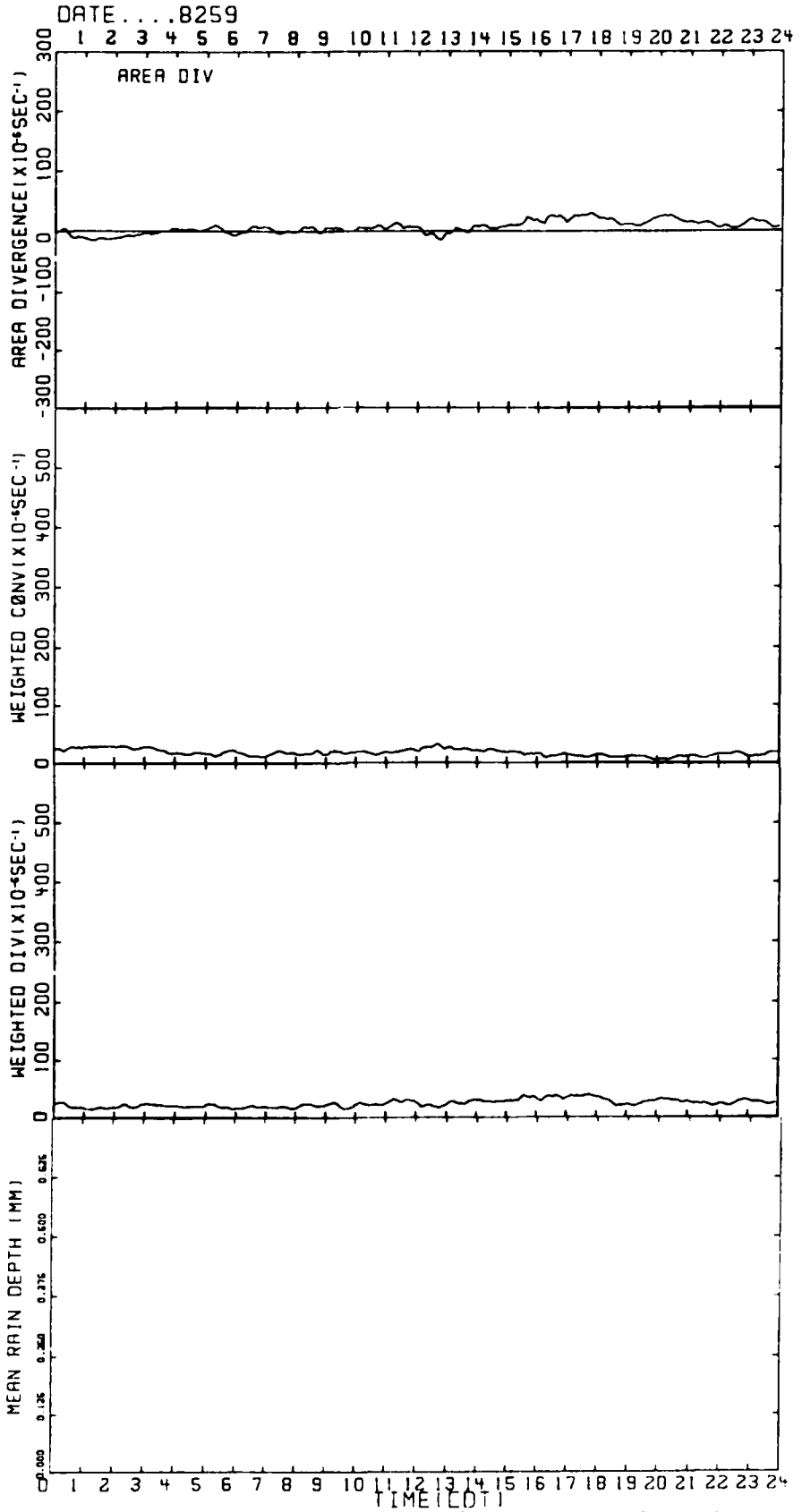

Figure 6. Time profiles of total area divergence, weighted convergence, weighted divergence, and area rain depth for 25 August 1979.

between the beginning of convergence to peak convergence. The Florida work described a convergence event as any sustained change in total area divergence less than $-25 \times 10^{-6} s^{-1}$ for more than 10 min. To filter noise from the data, this definition was applied to a three-point running mean (15-min average) of total area divergence. This event criterion has been applied to the Illinois data for comparison. The same basic description of a convergence event was also used for weighted convergence.

c. Statistical Relationships

(1) Total Area Divergence

All events are determined only by the total area divergence and weighted convergence time profiles. No distinction is made as to how convergent cells are situated in the mesonetwork. Table 1 gives the times of beginning convergence, length of the event, and total area rainfall for 13 and 14 July (Figs. 3 and 4), taking into account the -25×10^{-6} s^{-1} criterion. The most apparent events are at 1435 CDT on the 13th and at 0115 and 0540 CDT on the 14th. These three events show the classic sinusoidal pattern associated with the increase of convergence followed by divergence related to outflow and precipitation. Notice that the backside of the outflow is not considered an event.

Table 2 summarizes the results of total area divergence versus area rainfall for the VIN 1979 project. For the entire ensemble, there were 106 convergence events meeting the $-25 \times 10^{-6} s^{-1}$ criterion. Forty-four of the convergence events had rainfall,and the average was 1.53 mm per event. During the 33 study days, 86% of the total rainfall that occurred was reflected in some manner in the total area divergence. The average change in total area divergence per event is $-45 \times 10^{-6} s^{-1}$. The correlation coefficient (r) between convergence and rainfall was -.50; the F ratio was 34, and the

Table 1. Convergence events associated with total area divergence for the days shown in Figs. 3 and 4.

Date	Time of initial convergence(CDT)	Length of event(min)	Maximum change in convergence ($x10^{-6}s^{-1}$)	Total area rain (mm)
13 July	0655	70	30	0.0
	1435	60	114	7.4
	1815	45	37	.0003
	1935	50	35	0.0
14 July	0115	50	113	8.1
	0540	50	131	9.8
	0900	40	41	.2
	1310	50	37	0.0
	1715	40	32	.1
	1805	40	32	.0062
	2020	40	40	0.0

Table 2. Total area divergence versus rainfall based upon VIN 1979 mesonetwork data.

Criteria	No. of cases	Rain events	$\overline{\text{Rain}}$ (mm)	$\overline{\Delta DIV}$ ($\times 10^{-6} s^{-1}$)	Rain misses	$\overline{\text{Rain/miss}}$ (mm)	r	F ratio	Sig
All	106	44	1.53	-45	28	.97	-.50	34	<.001
RH<50%	23	4	.01	-35	3	.84	.06	.07	.79
50%≤RH<65%	45	19	1.52	-48	14	.57	-.57	20	<.001
RH≥65%	38	21	2.45	-48	11	1.52	-.39	7	.02
SI>2	35	9	.39	-38	5	.51	-.04	.05	.83
-1<SI≤2	49	18	.81	-46	16	1.12	-.47	13	.001
SI≤-1	22	17	4.92	-57	7	.97	-.52	7	.01
K≤22	28	5	.02	-33	7	.44	.15	.56	.46
22<K<29	21	8	1.54	-41	0	.0	-.11	.25	.62
K≥29	57	31	2.26	-53	21	1.15	-.50	19	<.001
V_{1-10}>5 m s^{-1}	67	31	2.15	-48	19	1.29	-.46	18	<.001
V_{1-10}≤5 m s^{-1}	39	13	.45	-41	9	.31	-.73	42	<.001

significance (Sig) of the corelation occurring from an uncorrelated population was less than 0.1%. Notice that 28 rain periods were not detected in the total area divergence time profile. The average rain per miss was .97 mm.

As found in south Florida, the convergence-rainfall relationships in Illinois are weak if examined without the aid of other meteorological factors. Therefore, the convergence-rainfall data are subdivided according to parameters such as moisture, stability, and winds to improve the statistical results. These parameters are obtained from 12-h upper-air reports at Salem and Peoria, Illinois, and the convergence events are grouped in time according to these observations. Since the VIN mesonetwork is approximately midway between the two upper-air stations, each parameter is the average value determined by the two locations.

The population is then subdivided according to middle-level relative humidity, that is, an average relative humidity between 850 and 500 mb. The best correlation (-.57) was found for the middle-range relative humidity (50% $\leq$ RH < 65%); 42% of the events (19 for 45) had rain. When the relative humidity was >65%, 55% of the events (21 of 38) had rain, and the amount was almost twice that when relative humidity was in the middle range. The correlation coefficient dropped to -.39, showing that the triggering mechanisms that caused the precipitation may not entirely lie in the surface wind field. For low relative humidities, only four events had rain with an expected very low correlation.

The ensemble is then subdivided according to the Showalter index, which is determined by lifting an air parcel from 850 mb dry-adiabatically to saturation, then moist-adiabatically to 500 mb. The index is the algebraic difference between the 500 mb temperature and the parcel temperature. Table 2 shows low rainfall and weak convergence with high stability indices.

Correlation is also low. When the stability index is ≤ -1, 6 times more rainfall occurs when compared with the middle range of stability indices ($-1 < SI \leq 2$). When instability is greatest, 17 events out of 22 had rain, making the strongest correlation between convergence and rainfall.

The K index is the next parameter examined. The K index measures thunderstorm potential based on lapse rate, the moisture content of the lower atmosphere, and the vertical extent of the moist layer. The higher the K, the greater the chances for thunderstorm activity. When K is greater than 28 (Table 2), 1 1/2 times more precipitation occurs, and convergence is greater than when K is between 23 and 28. The lower the K, the weaker the correlation between convergence and rainfall.

So far, when middle-level RH <50%, SI > 2, and K < 23, then very little rain occurs. For forecasting purposes, these are no-rain conditions. Under operational situations, these meteorological parameters can be updated every 12 h by nearby rawinsonde reports, and the user agency can be given a general rain/no-rain forecast at that time. When conditions warrant a rain forecast, then the user can expect to be notified 30-60 min before significant precipitation will occur, through the use of the total area divergence profile.

In FACE 1975, much more precipitation occurred when the low-level wind speed was small or when the systems moved very slowly. The mean vector wind speed is the vector-averaged speed between 1000 and 10,000 ft (V_{1-10}). The Illinois ensemble was divided according to $V_{1-10} = 5$ m s^{-1}, the same criterion as for Florida. When the wind speed was weak, only 33% of the events (13 out of 39) had rain, and the average was 0.45 mm per event. The correlation was quite good at -.73. When the wind speed was stronger, precipitation was 4 1/2 times more per event and convergence increased only slightly. Therefore,

there is a difference between the relations in south Florida and Illinois. The inherent cause for this difference between the weak and stronger speeds is probably the close proximity of the high pressure ridge in Illinois. The closer the mesonetwork in Illinois was to the center of the ridge, the slower the low-level wind speeds and the less the likelihood of a thunderstorm because of subsidence and resulting stable, dry conditions. If it did occur the thunderstorm was of the airmass type and not related to the stronger, more intense baroclinic systems associated with frontal systems, which, of course, would be associated with stronger winds aloft.

Statistically, it appears from Table 2 that the stability index is the best single way to divide the data. The wind criteria did a fine job, also, but only divided the data two ways. Some loss in significance occurs with the stability index criteria when the ensemble is divided three ways.

Fig. 7a-d shows the results of the convergence-rainfall regression equations subdivided according to relative humidity, stability index, K-index, and low-level wind speed. Recall that these equations as developed are highly dependent on area and region. Under stable and dry conditions, essentially a no-rain forecast can be made. Notice that when the middle-level relative humidity is between 50% and 65% (Fig. 7a), there is a greater chance for heavy precipitation than when the relative humidity is greater than 65%. The rationale for this is that layered clouds are usually present with very high middle-level humidities and the chance for moderate convective events due to weaker surface heating is less.

The Showalter index (Fig. 7b) appears to balance the data quite well; the positive indices predict little rainfall, and the negative indices predict larger amounts of precipitation. The K-index (Fig. 7c) reflects the findings

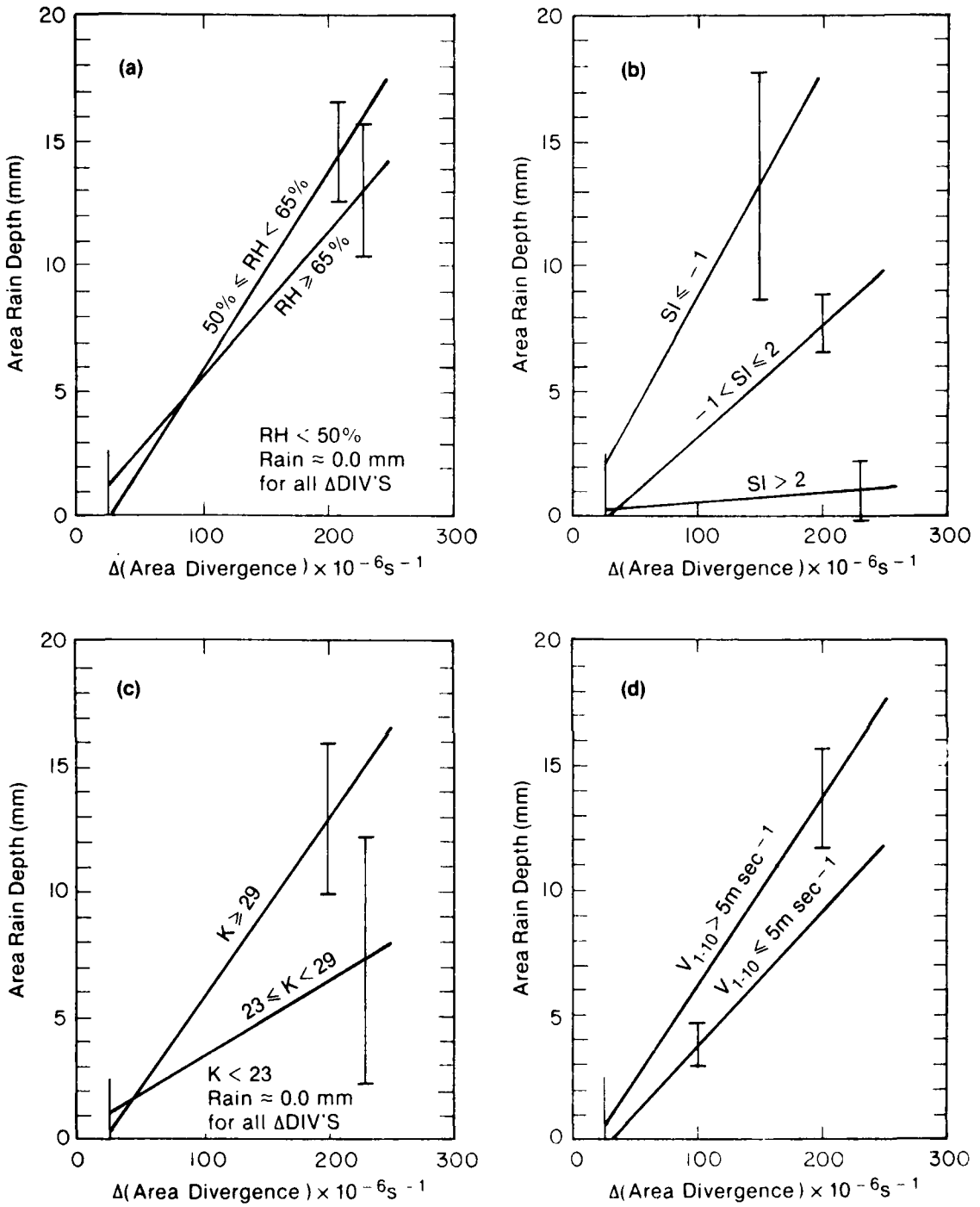

Figure 7. Linear regression for total area divergence versus area rain depth for VIN 1979. 95% confidence limits are included. Divisions are according to (a) middle-level relative humidity; (b) stability index; (c) K-index; (d) low-level wind speed averaged between 1000 and 10,000 ft.

of the stability index. Finally, Fig. 7d is indicative of the variability of precipitation associated with changes in winds aloft.

All the parameters above, with the exception of low-level wind speed, were subjected to a multiple linear regression scheme together with total area divergence, to predict precipitation. For the entire ensemble of total area divergence events only an increase in correlation coefficient from -.50 to -.57 was found, explaining only a 7% increase in the variance. This exercise revealed that the correlation between total area divergence and rainfall far exceeded the correlation between the three other parameters and rainfall. The Showalter index, K-index, and middle-level relative humidity were related individually to the rainfall events. It was discovered that the correlation ($r = -.30$) between the Showalter index and rainfall was best, and the K-index ($r=.26$) was second.

Table 3 gives the time in minutes between convergence and rain milestones. The time between beginning convergence and initial rainfall is only 5 min, which is strikingly different from the 35-min average in Florida. The reason is that many of the Illinois convective systems are mature as they move into the VIN network. The gust front enters the western edge of the network together with its associated convergence followed directly by beginning rain. In Florida, a majority of the convective systems develop almost in place. The heavier precipitating systems are slow moving. Therefore, the convergence builds in place followed by divergence and resulting precipitation.

The real nowcasting tool developed in this study and in Florida requires that the difference in divergence between beginning convergence and maximum convergence be computed so that the amount of rainfall be known shortly before the actual occurrence. The time between maximum convergence and rain maximum

Table 3. Time in minutes between convergence and rain milestones based upon VIN 1979 mesonetwork data.

	Time (min)		
	Begin convergence and initial rain	Maximum convergence and rain maximum	Begin convergence and rain maximum
Total Area Divergence	5(27)	23(48)	69(45)
Weighted Convergence	5(25)	37(29)	85(35)

* Standard deviations are in parentheses.

is crucial, and during this period the rain forecast must be disseminated to the potential user. In Illinois, the average time between maximum convergence and maximum rain is 23 min. This is again a reduction from south Florida (38 min). Since the events vary widely in size and duration, the standard deviations are quite large.

(2) Weighted Convergence

Weighted convergence filters any effects of positive divergence from total area divergence. The definition of weighted convergence was given in section 3a. One of the shortcomings of weighted convergence is the requirement of an inner grid of wind stations within the mesonetwork, whereas total area divergence can be determined with wind sites located only along the periphery.

Table 4 summarizes weighted convergence and its relationship to convective rainfall. In the total ensemble, only 45 cases met the criterion of 25×10^{-6} s^{-1} for 10 min or more as compared with 106 cases for total area divergence. This is quite intriguing since the south Florida sample sizes for area divergence and weighted convergence were almost identical. But, in Illinois, weighted convergence has filtered out the weaker and less important

Table 4. Weighted convergence versus rainfall based upon VIN 1979 mesonetwork data.

Criteria	No. of cases	Rain events	$\overline{Rain}$ (mm)	$\overline{\Delta DIV}$ ($\times 10^{-6} s^{-1}$)	Rain misses	$\overline{Rain/miss}$ (mm)	r	F ratio	Sig
All	45	27	3.48	50	45	.75	.50	14	<.001
RH<50%	6	1	.001	34	5	.53	-.12	.06	.83
50%<RH<65%	22	14	3.08	53	20	.50	.70	19	<.001
RH>65%	17	12	5.23	51	20	1.05	.19	.55	.47
SI>2	8	2	.34	37	12	1.12	-.43	1.3	.29
-1<SI<2	20	12	2.44	47	23	.47	.30	2	.19
SI<-1	17	13	6.17	59	10	.95	.54	6	.03
K<22	4	1	.002	36	10	.35	-.22	.10	.78
22<K<29	8	3	2.69	36	6	1.79	.86	17	.01
K>29	33	23	4.10	55	29	.67	.46	8	.01
V_{1-10}>5 m s^{-1}	36	21	3.84	49	30	1.01	.48	10	.003
V_{1-10}<5 m s^{-1}	9	6	2.05	53	15	.22	.82	14	.01

events. Sixty percent (27 out of 45) of the events had rain. The 3.48-mm average rainfall per event means that 82% of the total rainfall during this 33-day study was reflected in the weighted convergence.

When the ensemble is subdivided, the dryer and less moist subdivisions have too few samples making the groupings statistically insignificant. Nevertheless, the results resemble those of total area divergence. Figs. 8a-d present the regression lines for each meteorological parameter. Statistically the wind criterion best separates the data but it uses only two subdivisions. Stability index is second, using three subdivisions, and it separates the groups more proportionately.

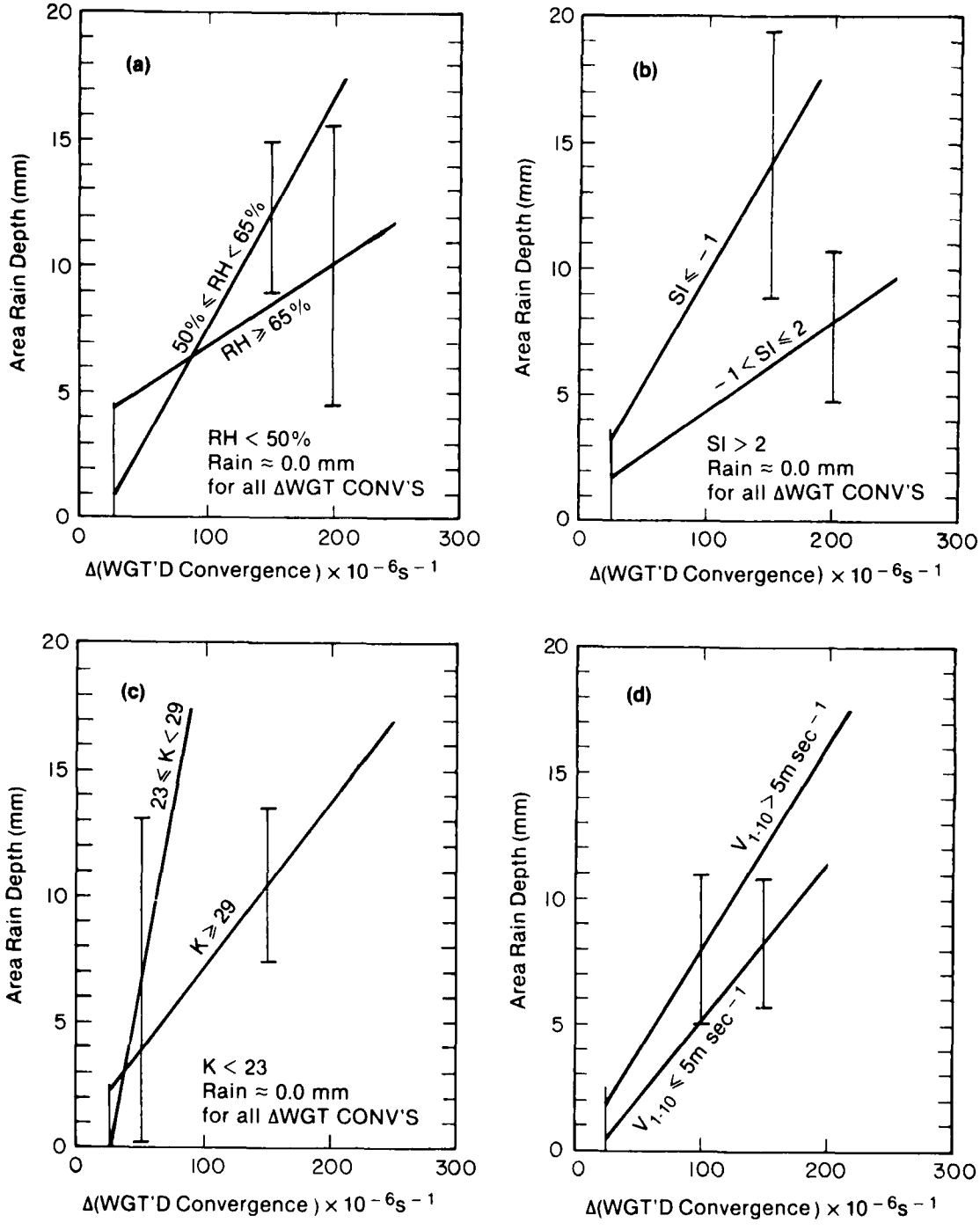

Figure 8. Linear regression for weighted convergence versus area rain depth for VIN 1979. 95% confidence limits are included. Divisions are according to (a) middle-level relative humidity; (b) stability index; (c) K-index; (d) low-level wind speed averaged between 1000 and 10,000 ft.

The time between beginning convergence and initial rain is about the same as for total area divergence (Table 3). The times between the maximum convergence and maximum rain and the beginning convergence and maximum rain have increased, since only the stronger events have been recorded by weighted convergence.

d. Effects of Low-Level Wind Direction

Table 5 examines convergence and rain events when related to mean low-level wind direction between 1000 and 10,000 ft. For the two sectors, 340° through 090°, and 090° through 180°, very few convergence and rainfall events occur. The one rain event totaling greater than 1 mm had a mean low-level wind direction of 145°. Essentially, a no-rain forecast can be made between 340° and 140°. The primary direction for convective activity is from the southwest, but, surprisingly, significant events (>1 mm) occurred with a mean low-level wind direction of 270° through 340°. When an operation of this nature is implemented, climatology of the type discussed here must be available. Even more important, at least one convective season must be used to develop the convergence-rainfall statistics peculiar to the size and locale of the region involved.

e. Convective Outflow Versus Area Rainfall

Byers and Braham (1949) found that an area of heavy rain at the surface coincides with an area of strong divergence in the surface winds. Correlation coefficients of .98 and .91 were found when nine storms perfectly situated in their upper-air network in Ohio and nine storms in Florida were studied. In the VIN study, total area divergence and weighted divergence associated with the outdraft are related to area rainfall. Total area divergence when related to the outflow is defined as the maximum change in divergence, beginning at maximum convergence and continuing to the maximum in divergence. For weighted

Table 5. Convergence and rain events subdivided according to mean low-level wind direction between 1000 and 10,000 ft for total area divergence and weighted convergence.

Sector	Convergence events	Rain events (>1 mm)	Rain events (<1 mm)	Rain events missed (>1 mm)	Rain events missed (<1 mm)
TOTAL AREA DIVERGENCE					
340°-090°	4	0	0	0	1
090°-180°	12	1	0	0	1
180°-270°	65	17	16	2	10
270°-340°	25	3	7	4	10
WEIGHTED CONVERGENCE					
340°-090°	1	0	0	0	1
090°-180°	2	1	0	0	1
180°-270°	34	15	6	3	23
270°-340°	8	3	2	3	14

divergence, it is the maximum change in divergence from the quiescent value to the peak value that occurs during the event. Figs. 3 and 4 show three outflows that appear as peaks in both the weighted divergence and total area divergence profiles.

Outflow divergence is not a predictor of precipitation because the divergence is an effect and result of both the downdraft and precipitation. It is understandable, however, that there should be a better relationship between the outdraft and rainfall than between inflow and rainfall since the precipitation causes the downdraft, which in turn causes the horizontal outflow at the surface. The assumption made here is that the outflows will have precipitation. The correlation between initial convergence and precipitation will be less since all the roots of the inflow may not be at the surface.

Table 6. Total area divergence associated with convective outflow as related to area rainfall (>0.5 mm) based upon VIN 1979 mesonetwork data.

Criteria	No. of cases	$\overline{RAIN}$ (mm)	$\overline{\Delta DIV}$ ($x10^{-6}s^{-1}$)	r	F ratio	Sig
All	29	6.29	102	.65	20	<.001
RH<50%	2	1.21	13	*	*	*
50%≤RH<65%	13	5.59	115	.90	48	<.001
RH≥65%	14	7.66	103	.22	.59	.46
SI>2	5	3.07	42	.99	142	.001
-1<SI≤2	10	5.38	92	.26	.56	.48
SI≤-1	14	8.08	131	.68	11	.01
K≥29	22	6.72	110	.58	10	.01
K<29	7	4.92	78	.95	44	.001

*Insufficient data

Only precipitation events totaling >0.5 mm of area rainfall were examined. Twenty-nine rain events met this criterion. Tables 6 and 7 give the statistical relationships developed for total area divergence and weighted divergence. As a whole, the correlation coefficients improve approximately .15 over the convergence-rainfall statistics presented in section 3c. These still remain about a tenth lower than the Florida results for convective outflow (Watson et al., 1981). Essentially, the more unstable and moist the atmosphere, the more the divergence and precipitation. However, this is not the case for very moist (RH ≥ 65%) conditions, where larger precipitation totals are coupled with weaker divergence values. The wind speed subdivision was deleted from the tables because only three samples were included in the group when low-level wind speeds were <5 m s^{-1}.

Table 7. Weighted divergence associated with convective outflow as related to area rainfall (>0.5 mm) based upon VIN 1979 mesonetwork data.

Criteria	No. of Cases	$\overline{RAIN}$ (mm)	$\overline{\Delta DIV}$ ($x10^{-6}s^{-1}$)	r	F ratio	Sig
All	29	6.29	62	.62	17	<.001
RH<50%	2	1.21	15	*	*	*
50%≤RH<65%	13	5.59	74	.87	35	<.001
RH≥65%	14	7.66	58	.21	.55	.47
SI>2	5	3.07	34	.90	12	.04
-1<SI≤2	10	5.38	52	.27	.65	.44
SI≤-1	14	8.08	79	.64	8	.02
K>29	22	6.72	63	.56	9	.01
K<29	7	4.92	60	.87	16	.01

*Insufficient data

4. Representativeness of Surface Divergence with Boundary-Layer Divergence

The purpose of this section is to examine the representativeness of the surface divergence field to boundary-layer divergence on a meso- β scale in Illinois. The main thrust of the work, so far, has been the prediction of convective precipitation based upon the evolution of total area divergence with time. It has been found that in some cases the relationship between total area divergence and precipitation does not hold true. In Florida, Watson and Blanchard (1982) found reasonably good correlations (>.6) between convergence and rainfall. Work in the VIN network has shown that the correlations drop another tenth when compared with south Florida. In Florida the triggering mechanism for convection is usually simple; differential heating between the water surfaces and the land mass create the lake- and sea-

Table 8. Boundary-layer classifications.

Category	Boundary-layer description
1	Convective: well-mixed boundary layer
2	Non convective: well-mixed layer but formed by mechanical mixing
3	Convective: well mixed layer with cumulonimbus present in or near pibal triangle
4	Boundary layer under influence of downdraft air from cumulonimubus
5	Other: boundary layer does not meet any of the categories above

breeze circulations. In the Midwest, the forcing mechanisms are varied, including large- and small-scale interactions, low- and middle-level disturbances, and surface heating, among others. Therefore, the actual key in relating convergence to the amount of precipitation may lie somewhere above the surface. These data are limited to low-level divergence determined by the VIN 1979 pibal triangle. The highly variable nature of boundary-layer divergence is shown under several different types of conditions. A statistical relationship between surface divergence and divergence at 50-m increments aloft is developed.

a. Boundary-Layer Classification

Thirty days with pibal data have been examined for this study. Each observation has been classified according to what appears to be the basic structure of the boundary layer in the 750 km^2 pibal triangle (see Fig. 1) at that time. A description of the five categories is given in Table 8. These classifications are based upon radiosonde observations, time lapse

photography, and radar information from the NWS WSR-57 surveillance radar located at Marseilles, Illinois.

Table 9 summarizes the correlation (r), number of samples (n), F ratio, and significance (Sig) of area divergence at each level with the surface divergence for the total ensemble and Types 1-4 boundary-layer classifications. These classifications are graphically represented in Fig. 9. The solid line is the mean profile of divergence with height (MSL). The dashed line is the correlation coefficient between surface divergence and divergence calculated at 50-m increments aloft.

The Type 1 boundary-layer classification is shown in Fig. 9a. This is a mean profile of divergence with height (MSL) of all Type-1 observations found in the 30-day pibal data set. Cloud conditions may be scattered or broken cumulus. Very little area convergence is observed because the smaller scale updrafts and downdrafts cancel each other. Correlations between surface divergence and divergence aloft show that the level most highly correlated with the surface is at 350 m MSL ($\simeq$ 150 m AGL), the level closest to the surface. The correlations then decrease steadily with altitude.

Fig. 9b shows the Type 2 divergence and correlation profile associated with mechanical mixing and high surface winds following, for example, a cold frontal passage. Cold air advection coupled with moderate low-level winds usually produces broken-to-overcast stratocumulus with bases at 200 to 500 m AGL. The divergence profile exhibits weak convergence through 450 m followed by a rapid increase in divergence, reaching a maximum at 1000 m. Difluence behind the cold front is probably responsible for this divergence maximum. The correlation profile again shows that the level closest to the surface is the most highly correlated level with the surface.

Table 9. Statistical relationships between surface divergence and divergence aloft at 50-m increments in the pibal triangle for 30 VIN study days.

HGT (m) MSL	Entire Ensemble r	n	F	Sig	Type 1 r	n	F	Sig	Type 2 r	n	F	Sig	Type 3 r	n	F	Sig	Type 4 r	n	F	Sig
SFC (=200mMSL)		258				193				32				18				11		
350	.47	252	72	<.001	.35	190	27	<.001	.75	30	37	<.001	.46	17	4	.06	.49	11	3	.13
400	.46	256	67	<.001	.33	192	24	<.001	.65	31	21	.001	.40	18	3	.10	.47	11	3	.14
450	.45	246	61	<.001	.33	189	22	<.001	.62	24	13	.001	.40	18	3	.10	.37	11	1	.26
500	.43	246	56	<.001	.32	189	21	<.001	.58	24	11	.003	.42	18	3	.08	.25	11	<1	.45
550	.40	231	42	<.001	.29	178	16	<.001	.53	21	7	.01	.42	18	3	.08	.14	10	<1	.69
600	.34	230	30	<.001	.23	177	10	.002	.49	21	6	.03	.41	18	3	.09	.04	10	<1	.91
650	.24	218	13	<.001	.20	168	7	.01	.41	20	4	.07	.15	17	<1	.56	.12	9	<1	.76
700	.19	218	8	.005	.18	168	5	.02	.27	20	1	.25	.13	17	<1	.61	.02	9	<1	.96
750	.13	203	3	.08	.16	159	4	.04	-.04	19	<1	.86	.13	14	<1	.67	.05	7	<1	.92
800	.11	203	2	.12	.16	159	4	.04	-.13	19	<1	.58	.16	14	<1	.59	-.03	7	<1	.96
850	.11	182	2	.14	.15	142	3	.08	-.28	17	1	.29	.54	12	4	.07	-.05	7	<1	.92
900	.11	182	2	.16	.17	142	4	.05	-.32	17	2	.21	.54	12	4	.07	-.07	7	<1	.89
950	.05	159	<1	.50	.17	128	4	.06	-.22	13	<1	.47	.76	7	7	.05	-.06	7	<1	.89
1000	.05	159	<1	.56	.19	128	5	.03	-.18	13	<1	.56	.75	7	7	.05	-.03	7	<1	.94
1050	.00	144	.000	.97	.19	115	4	.04	-.12	13	<1	.69	.74	6	5	.10	.51	6	<1	.30
1100	-.02	144	<1	.82	.19	115	4	.04	.01	13	.00	.96	.76	6	6	.08	.43	6	<1	.40
1150	-.05	131	<1	.54	.13	104	2	.20	.15	13	<1	.62	.67	5	2	.22	.39	6	<1	.45
1200	-.08	120	<1	.40	.11	97	1	.27	.27	10	<1	.45	.49	4	<1	.51	36	6	<1	.49
1250	-.11	116	1	.23	.09	96	<1	.39	.35	10	1	.33	M	M	M	M	.28	5	<1	.65
1300	-.17	[illegible]	3	.09	.00	85	.00	1.00	.40	9	1	.28	↓	↓	↓	↓	.31	5	<1	.62
1300	-.25	99	7	.01	-.10	82	<1	.38	.33	9	<1	.39					.21	5	<1	.73
1400	-.25	90	6	.02	-.10	75	<1	.38	.34	8	<1	.41					.13	5	<1	.83
1450	-.25	90	6	.02	-.12	75	1	.32	.21	8	<1	.62					.16	5	<1	.79
1500	-.30	77	7	.01	-.17	63	2	.20	-.07	7	<1	.89	↓	↓	↓	↓	.20	5	<1	.75

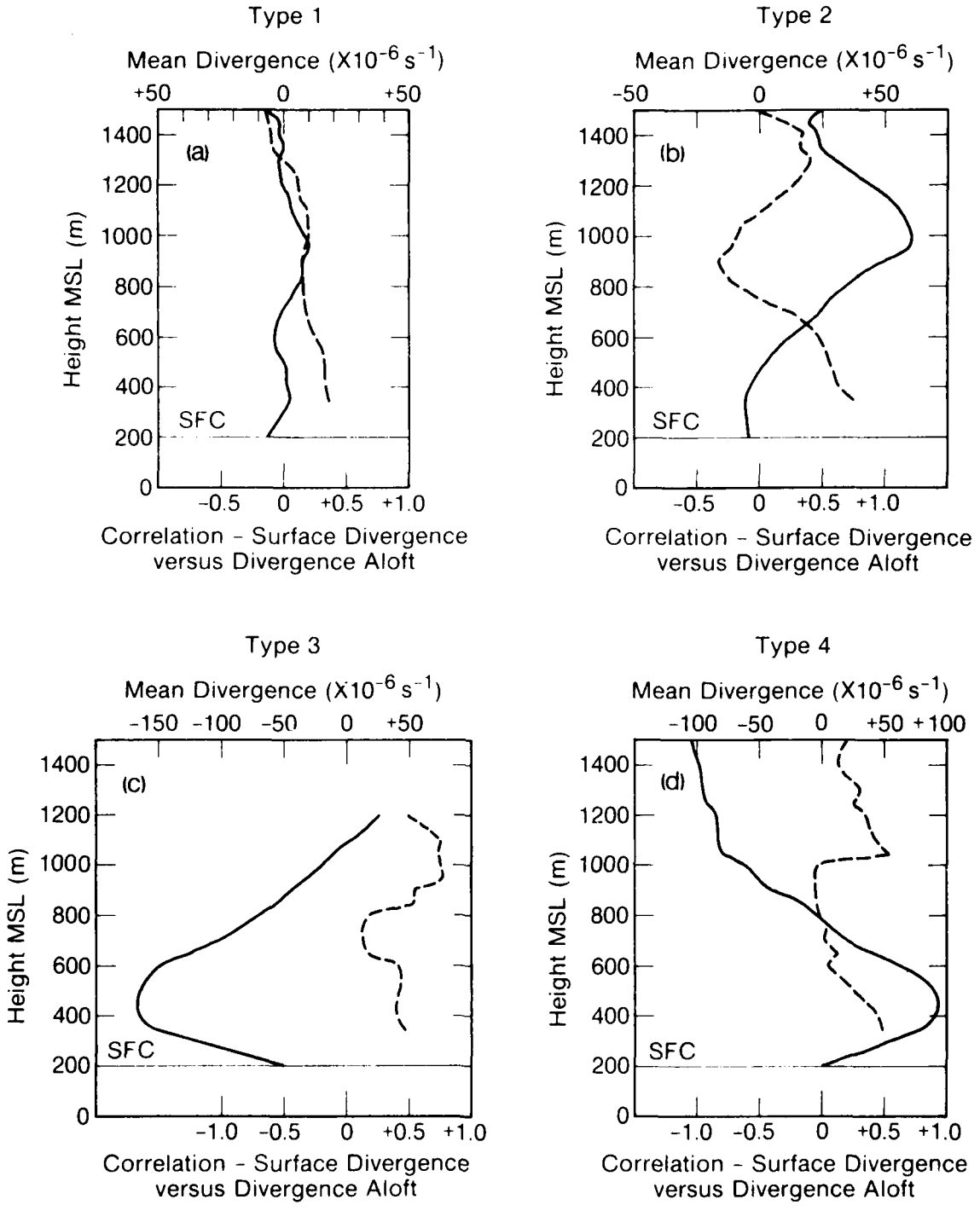

Figure 9. Mean profiles (solid lines) for boundary-layer classifications. Included are correlations between the surface divergence and divergence aloft at 50-m increments (dashed lines).

The Type 3 profile (Fig. 9c) is a well-mixed layer with developing cumulonimbus present, but downdraft air is not significantly influencing the pibal triangle. Convergence is depicted at the surface and reaches a convergence maximum at 450 m (MSL) or 250 m (AGL). This maximum in convergence is some 3.5 times the surface value. Upon examination of individual Type 3 pibal divergence profiles, it was not unusual to see a maximum of 4 to 6 times the surface value; on 17 August at 1630 CDT the maximum was 15 times the surface value. Byers and Hull (1949), using winds aloft every 1000 ft around developing cumulonimbus, found a convergence maximum at 2000 ft and a minimum near 4000 ft, but no crossover from convergence to divergence as found here. Recent work by Brown and Hanson (1978), using FACE 1975 data, found that for a well-mixed convective boundary layer, a good assumption was that divergence increased logarithmically to 1.5 times the surface value at 100 m AGL and then remained constant throughout the remainder of the boundary layer.

Type 4 (Fig. 9d) depicts convective outflow conditions. A divergence maximum is found at 250 m AGL, followed by a rapid decrease in divergence until it reaches a crossover at 600 m AGL, above which convergence is dominant. This agrees with the finding of Byers and Hull (1949) in Florida, that when the downdraft had developed, divergence decreased monotonically from near the surface to zero at the average altitude of 800 m.

In both the Type 3 and Type 4 cases the presence of a constant stress layer within the first 250 m appears to be approximated by the logarithmic wind law. This has been found to be the case with Oklahoma gust fronts (Goff, 1975). Above the constant stress layers both the inflow and outflow cases reveal highly sheared environments. Under the well-mixed convective regime,

wind shear is small, which agrees with the results of Arya and Wyngaard (1975) when baroclinic effects are present.

Upon examination of all the correlation profiles, it is apparent that the surface and the level closest to the surface (150 m AGL) are the most highly correlated. Maximum convergence and divergence in the Type 3 and Type 4 profiles occur at 250 m AGL (450 m MSL). The correlation at this level (see Table 9) with the surface decreases significantly in both cases, from .46 to .40 (Type 3) and from .40 to .37 (Type 4). Type 1 has by far the largest number of samples; Type 3 and Type 4 have very few. Type 2 shows the best correlation (r=.75) between the surface and 350 m MSL.

When it was possible, an averaged divergence in the vertical was determined for 150 to 800 m AGL (350 to 1000 m MSL) for each sounding. This value was then related to the surface divergence at that time. For 154 pibal ascents, a correlation coefficient of .26 was found between the surface divergence and the mean boundary-layer divergence. The majority of cases (125) were Type 1 profiles. It appears from these results that mean divergence data in the vertical would not be helpful as a predictive tool.

b. Case Examples

(1) Fair Weather

Illinois was under the influence of high pressure on 18 July 1979. The high pressure center at the surface through 850 mb was located over the upper Mississippi valley. Generally northeast flow and clear skies were recorded across the mesonetwork. Fig. 10a is a plot of the sounding information reported at 1900 CDT at Peoria, Illinois. A very well defined mixed layer up to 2000 m is shown with a relatively strong capping subsidence layer above. A time-height profile of the divergence in the pibal triangle (see Fig. 1) from 1000 to 1500 CDT is found in Fig. 11. Also included in Fig. 11 is the

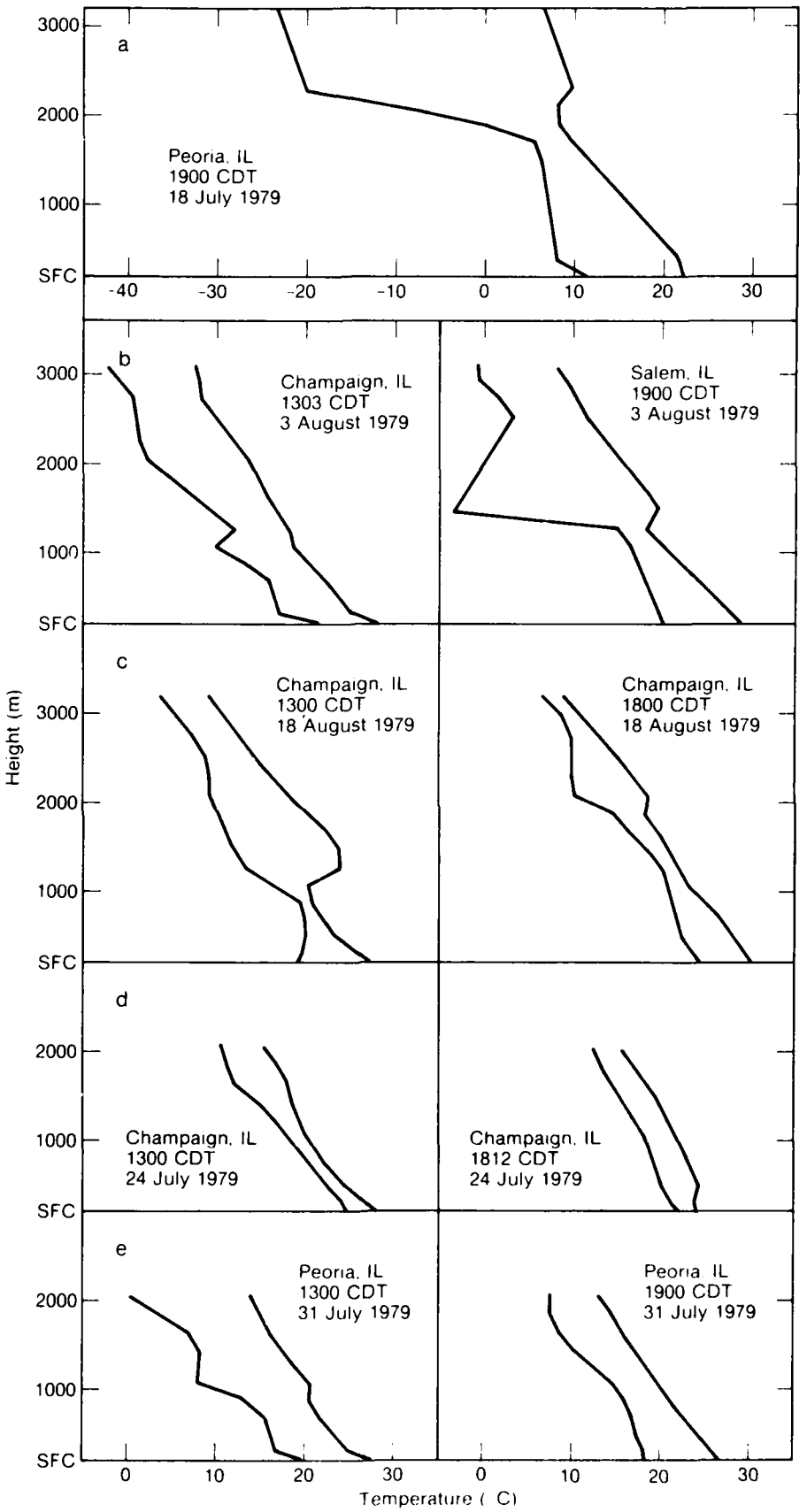

Figure 10. Low-level temperature-dewpoint sounding data for 18 July, 3 August, 18 August, 24 July, and 31 July 1979.

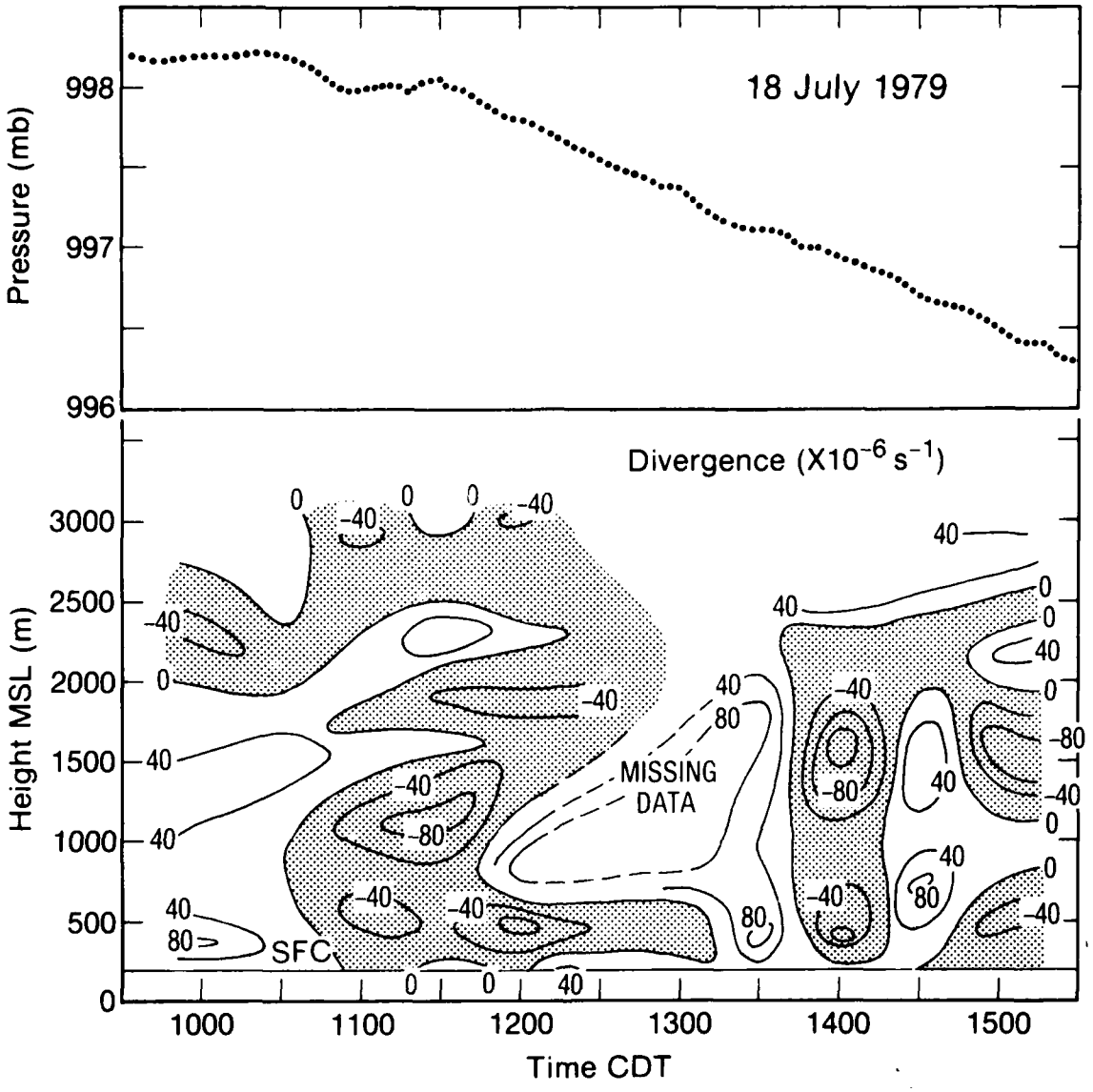

Figure 11. Divergence time-height profile and six-station mean-pressure profile for 18 July 1979.

averaged station pressure from the six PAM sites located in the triangle. Pressure shows the basic diurnal trend for this time of day. Divergence exhibits a couple of convergence episodes, but values are not large and do not persist.

On 3 August 1979 (Figs. 10b and 12), there was fair weather with somewhat more varying conditions. Illinois was wedged between two east-west stationary fronts. One which lay across Tennessee and Arkansas was cutting off moisture from the Gulf, while the other was near the U.S.-Canadian border. Conditions across the mesonetwork indicated generally moderate southwesterly flow at the surface and just a few widely scattered cumulus. Early-morning showers were reported in northwest Illinois. A region of dry air extended westward from the Ohio valley across extreme eastern Illinois and down through southern Illinois. At middle levels, Illinois was between two troughs, one in the Ohio valley and the other in Nebraska. Soundings (Fig. 10b) at 1330 CDT at Champaign and 1900 CDT at Salem reveal the development of a subsidence inversion at 1100 m MSL. The time-height divergence profile (Fig. 12) shows a weak but persistent divergence zone between 1500 and 2000 m MSL throughout the entire afternoon. Convergence is found above 2000 m. In the boundary layer (below 1200 m), nothing of a lasting nature is detected. Plumes of convergence are followed quickly by divergence.

(2) Disturbed Weather

(a) 18 August 1979

On 18 August 1979, a frontal system was slowly slipping southward near the Illinois-Wisconsin border. Southwesterly flow dominated the mesonetwork; early morning shower activity ended by 1000 CDT. Aloft, a short-wave trough over the north-central Great Lakes region was moving eastward and flattening the middle-level ridge. A confluent zone associated with the frontal system

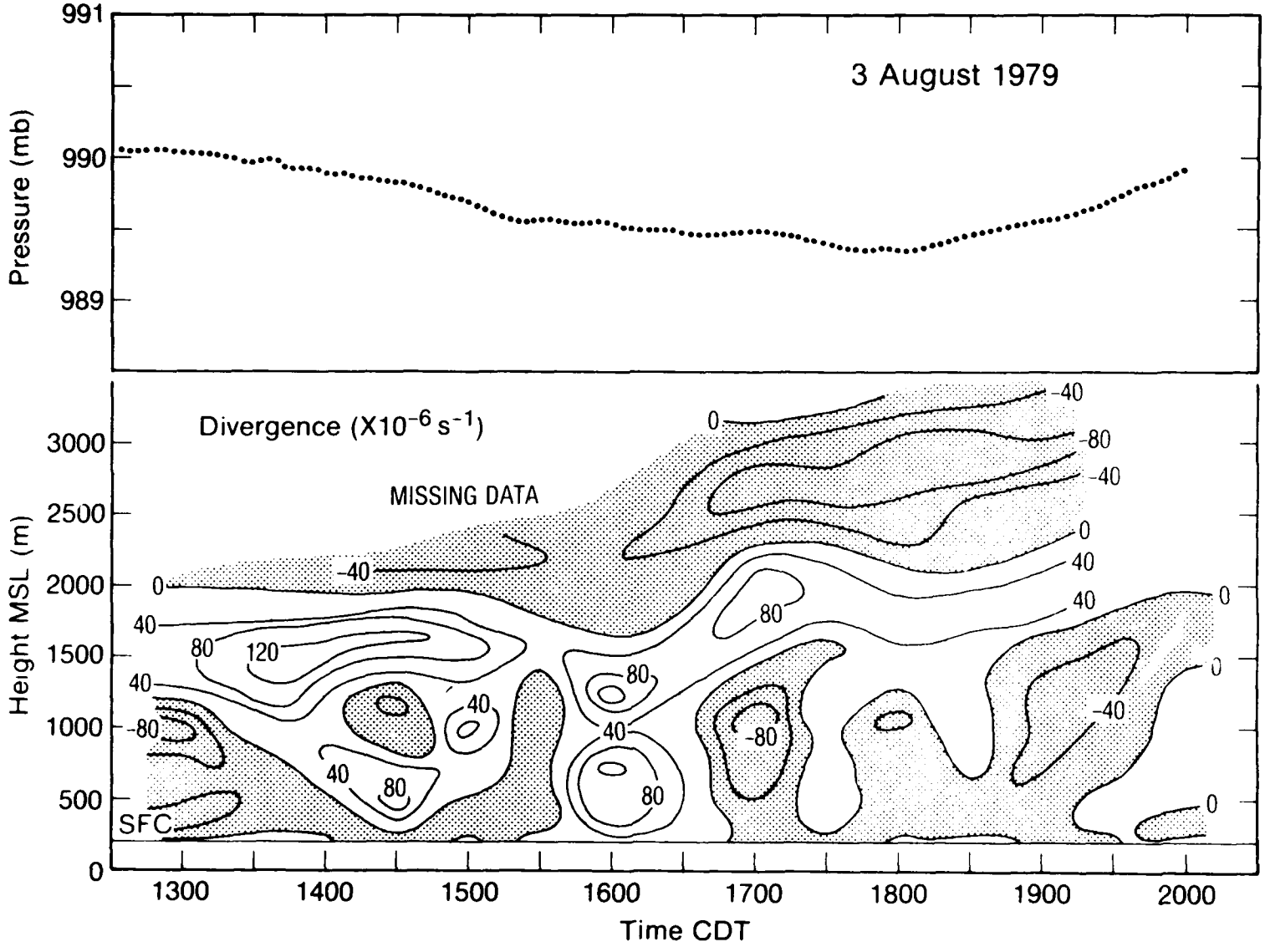

Figure 12. Divergence time-height profile and six-station mean-pressure profile for 3 August 1979.

at 850 mb was situated over the Illinois-Wisconsin border. Abundant available moisture aloft ($\overline{RH} > 70\%$) and close to 7.2 mb h^{-1} NMC vertical velocities were found over the area at 1900 CDT.

The mesonetwork was dominated by scattered cumulus through most of the afternoon. Fig. 10c shows the soundings recorded at 1300 and 1800 CDT at Champaign. On the early sounding, a well-mixed boundary layer is capped by a strong inversion at 1000 m MSL. But by 1800 CDT, the boundary layer appears to have become much warmer and deeper, and the inversion has weakened significantly.

Fig. 13 shows the time-height and surface data for 18 August. At the top of Fig. 13 is a time series of pressure. The solid line represents data from PAM-16 located in the middle of the pibal triangle (Fig. 1). The dotted line is a six station average of PAM sites located in the triangle. At the bottom of Fig. 13 is a time plot of θ_e for both PAM-16 and averaged data. Area rainfall in the VIN network is also plotted at the bottom of Fig. 13.

The time-height profile of divergence shows persistent boundary-layer convergence beginning at 1500 CDT. A large increase in inflow starts after 1800 CDT. The maximum occurs at 1900 CDT coincident with the pressure minimum and the start of precipitation. The maximum in convergence occurs at 200 m AGL as shown in the averaged profiles (Fig. 9c). Notice the drop in θ_e as the outflow reaches the PAM-16 site. The averaged θ_e also shows a drop as outflow air spreads across the triangle. The maximum in rainfall at 1955 CDT also corresponds to the pressure maximum at 2000 CDT. This activity developed from a small east-west line of showers that formed north of the VIN network at 1700 CDT. The west side of the line extended and developed southwestward and moved across the network from 1900 to 2200 CDT.

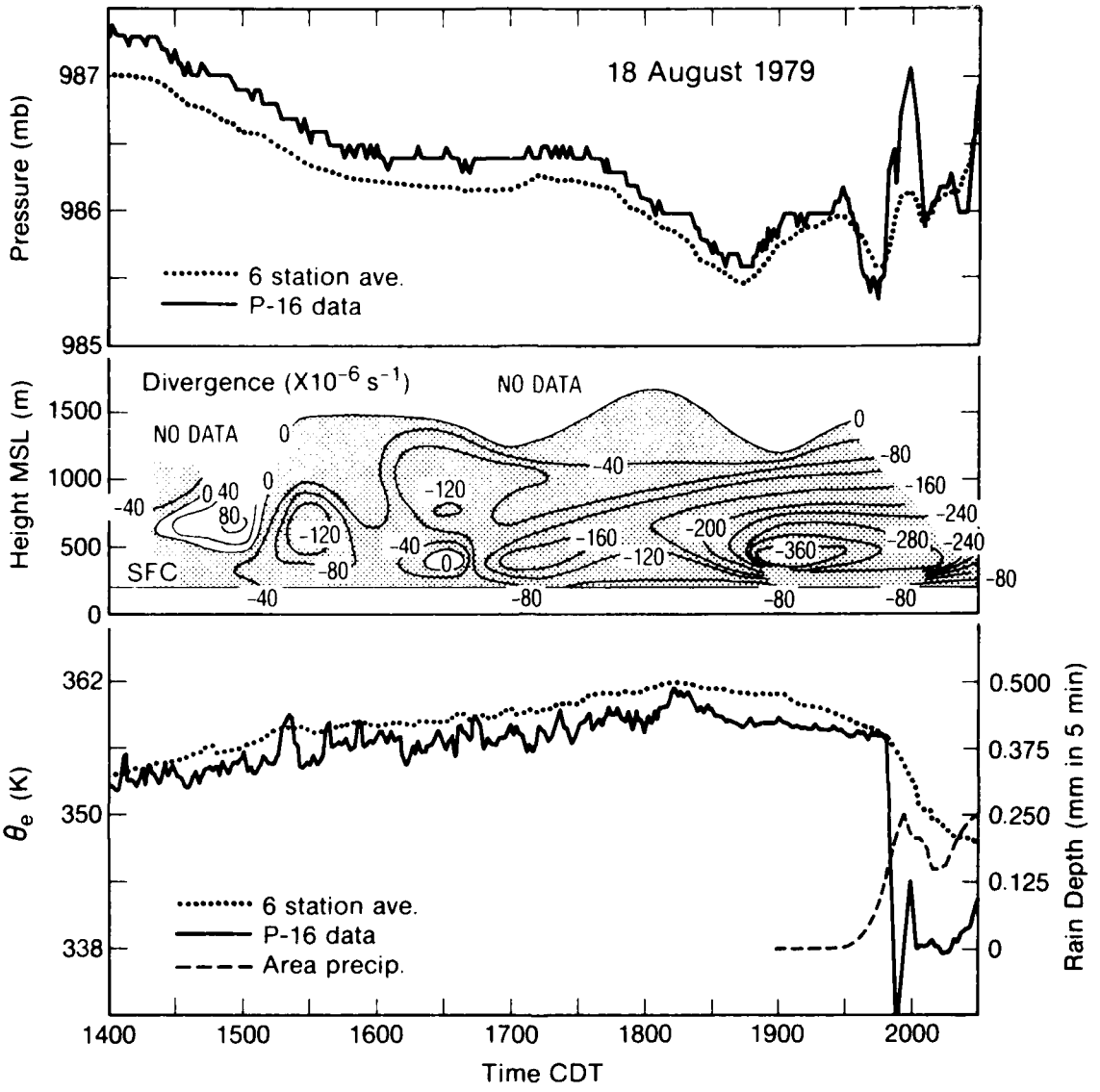

Figure 13. Divergence time-height profile, PAM-16 pressure and θ_e profiles, six-station mean-pressure and θ_e profiles, and mesonetwork rainfall for 18 August 1979.

(b) 24 July 1979

This day shows a moderate increase of mesoscale convergence followed by large values of divergence as outflow air and precipitation spread across the triangle. Synoptic conditions show a northeast-southwest cold front extending out of Canada into northwest Wisconsin and into central Kansas. The front is slowly moving southeastward, allowing south to southwest surface winds over Illinois. Tropical Storm Claudette is moving onto the east Texas Gulf coast. Aloft, there is south to southwest flow over Illinois. A distinct trough over eastern Iowa and Missouri extends into the center of Claudette. There is a fairly weak current at higher levels. Weak positive vorticity advection is occurring in conjunction with abundant amounts of moisture ($\overline{RH}$ = 85%) aloft.

The day is quite disturbed across the VIN network. Strong early-morning thunderstorm activity moves out of the area by 1200 CDT. The afternoon is dominated by small individualized cells of convection developing and dissipating rapidly. After 1900 CDT another fairly large complex moves eastward across the network. Fig. 10d shows the soundings at Champaign for 1300 and 1812 CDT. Very moist conditions are found on both soundings, and on the latter there is significant cooling at the surface due to outdrafts.

The chronology of events during the afternoon is depicted in Fig. 14. Organization is the key in the boundary layer where moderate values of convergence prevailed through most of the afternoon. The diurnal pressure fall is amplified somewhat by the retreating high-pressure ridge over the southeast United States and advancing mesoscale system after 1730 CDT. A weak outflow (1700 CDT) is seen at the surface as a small north-south line enters the pibal triangle. Significant downdraft air reaches the surface after 1830 CDT as evidenced by surface pressure and Θ_e time series. Rain has caused the end of the pibal data collection at 1800 CDT.

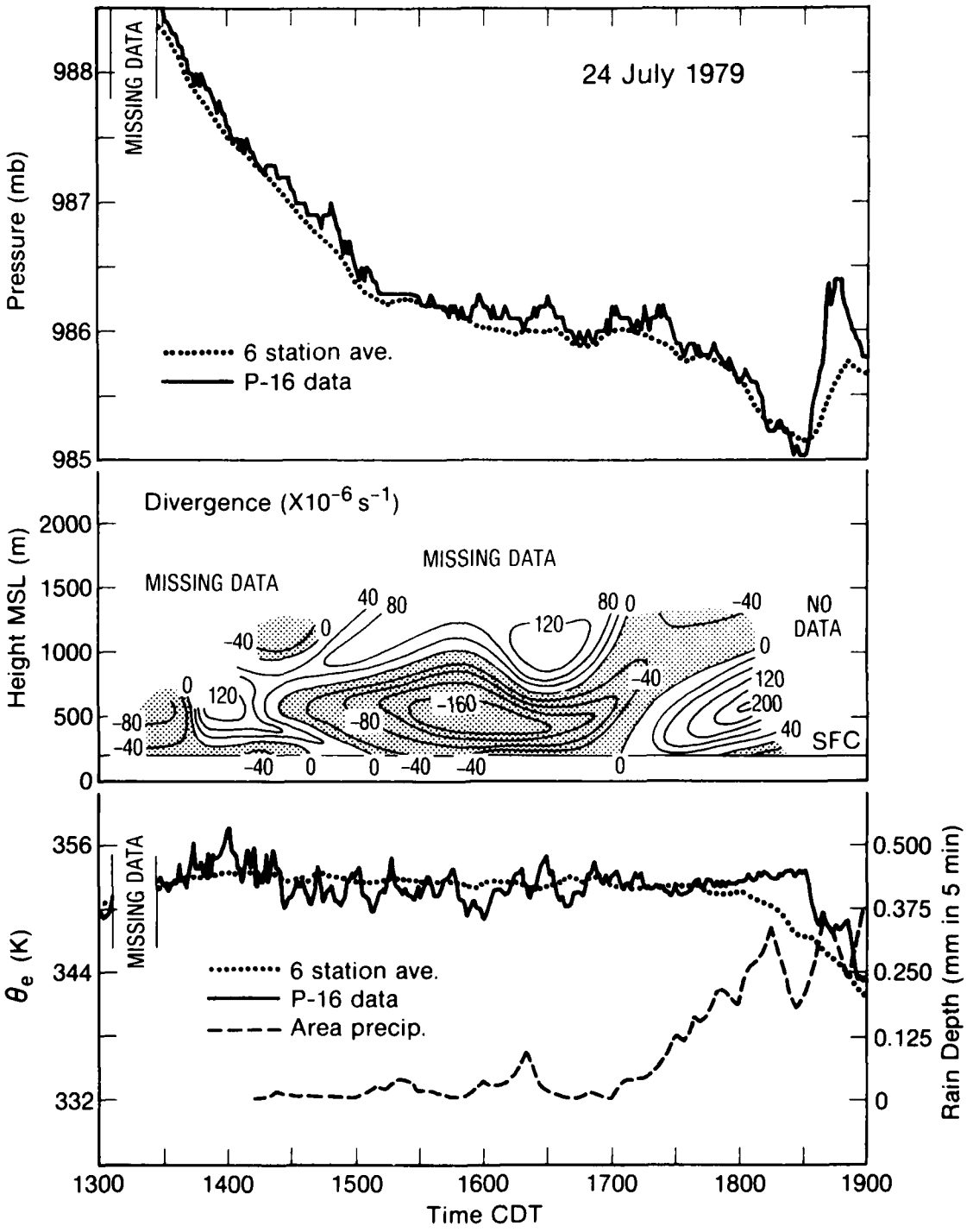

Figure 14. Divergence time-height profile, PAM-16 pressure and Θ_e profiles, six-station mean-pressure and Θ_e profiles, and mesonetwork rainfall for 24 July 1979.

(c) 31 July 1979

This day is of particular interest since a weak cold front traverses the mesonetwork during the late afternoon. Aloft, the mean relative humidity is greater than 70%, and upward vertical motion is weak. Very disturbed and violent thunderstorm activity had occurred during the previous evening, interspersed with periods of precipitation until 0700 CDT. Broken-to-overcast, middle and high clouds were observed all day, and rain fell briefly during the late morning and early afternoon. Little change can be noted in the low-level sounding data (Fig. 10e) for 1300 and 1900 CDT.

Divergence, rainfall, and thermodynamic profiles for 1400-2000 CDT can be seen in Fig. 15. Surface pressure appears to be very flat and holding steady after 1530 CDT. Θ_e does not show a decrease until after 1730 CDT. The divergence profile shows weak low-level convergence until a moderate pulse of divergence undercuts the convergence after 1800 CDT. A weak shower enters the western edge of the network at 1730 CDT, but it is hypothesized that the divergence is associated more with the passage of the front than with the light precipitation.

c. Summary

Ulanski and Garstang (1978) and Watson and Blanchard (1982) found that surface divergence is a good, but not excellent, indicator of convective rainfall. The study reported here has shown that the relationship between surface divergence and divergence aloft is not clear. The use of boundary-layer divergence alone appears to be encouraging. It was found that on nondisturbed days there was a noticeable lack of persistence in the divergence, both in the vertical and with time. But under disturbed conditions, persistent organization of the divergence aloft was always found. When cumulonimbus was present, convergence was dominant, and the

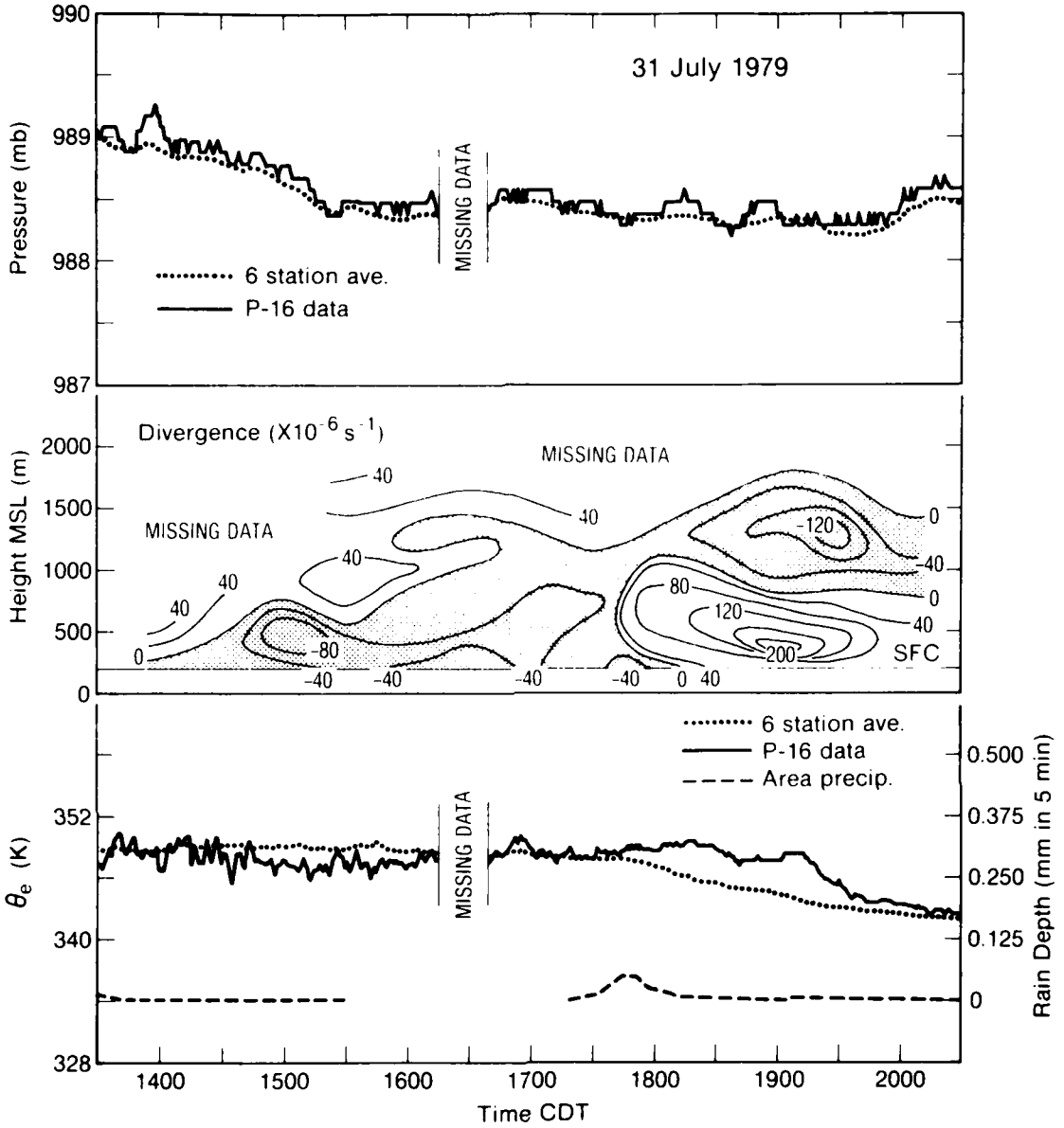

Figure 15. Divergence time-height profile, PAM-16 pressure and Θ_e profiles, six-station mean-pressure and Θ_e profiles, and mesonetwork rainfall for 31 July 1979.

maximum occurred at 250 m AGL. Under outflow conditions, a maximum in divergence was found at approximately the same level. It was also shown that the strength of the convergence associated with convection, and the divergence associated with precipitation and outflows, cannot always be detected precisely with the surface divergence. Surface frictional effects which are maximized with surface area divergence are resolved with the measurement of divergence aloft.

5. Illinois versus Florida

This convergence study was prompted by the work of Ulanski and Garstang (1978) who, using FACE 1971 and 1973 data, found readily identifiable convergence zones that precede the onset of precipitation. They related the convergence gradient with maximum point rainfall when cells of convergence had contours $\geq 600 \times 10^{-6}$ s^{-1} and persisted for 15 min or more.

The objective of this work has been to develop a relationship between convergence and rainfall on an area-wide basis. This was accomplished first by developing a technique in the relatively simple atmosphere of south Florida, then testing the hypothesis in a more complicated environment of the Midwest. The Florida study provided very encouraging results. For nowcasting, correlation coefficients between total area divergence and rainfall were .6. It was found that slow moving systems had 3 times the amount of rain with only a 30% increase in convergence, compared to the faster moving systems. When middle-level moisture was available, 2 1/2 times more precipitation was recorded for about the same amount of convergence than occurred during dry periods.

But, as found in section 3, the Illinois relationships are not as difinitive. The correlations have dropped a tenth when compared with south Florida. Systems in Illinois are not the slow movers that systems are in

Florida. In many instances, the systems are organized into squall lines or convective complexes. The lines are relatively fast moving (climatological average = 27 kn) from the west-southwest (Changnon and Huff, 1980). The associated convergence is along the outer fringes of the gust front, traveling as fast as the convective system itself. As shown in Table 3, rainfall begins about 5 min after initial convergence.

Figs. 16 and 17 present normalized convergence events developed for south Florida and Illinois. For normalization purposes, 0.0 represents beginning convergence and 1.0 is the end of the divergence or outflow, that is, when divergence returns to quiescence. Only convergence events with precipitation have been used. In FACE 1975, rain begins shortly before maximum convergence. Up until this time the mesoscale is feeding the system. When precipitation begins, convective-scale interactions begin and the requirement for mesoscale air lessens. A balance is found during maximum rainfall where there is no need for mesoscale air at all, so that total area divergence becomes zero. Finally, at maximum divergence, air is again passed back to the mesoscale. In Illinois, there appears to be more rainfall per event and the precipitation begins much earlier. More mature systems are entering the Illinois network, whereas the heavier precipitating systems develop and die in or very near the Florida network. Maximum rain occurs near zero total area divergence just as it did in south Florida. Total area divergence is much weaker in Illinois, principally because the Illinois network is twice as large as the FACE 1975 network. Recall that rainfall data in south Florida are estimated from radar. Since the reflectivity cone is approximately 1.5 km above the FACE mesonetwork, there is a possible 5-10 min lag time between radar estimated rainfall and actual precipitation recorded at the surface.

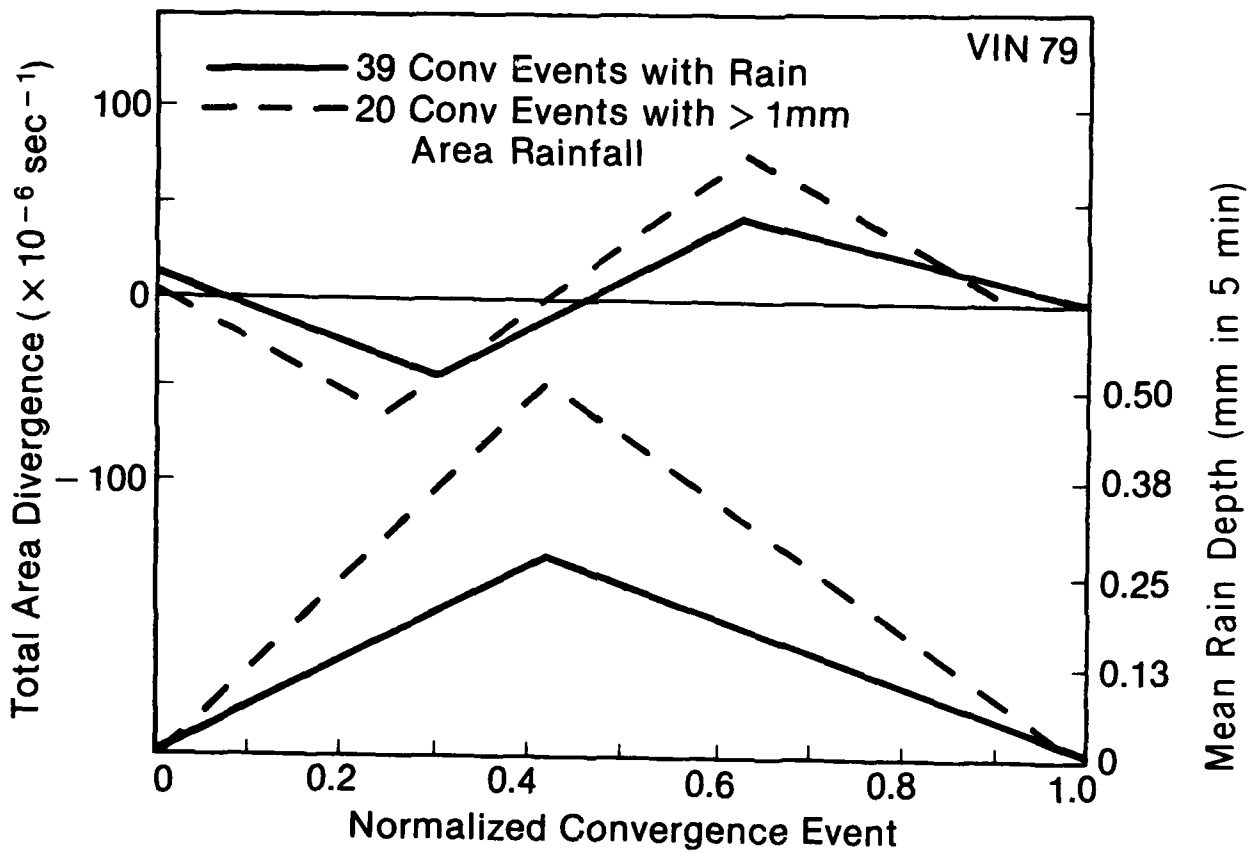

Figure 16. Normalized convergence event for VIN 1979.

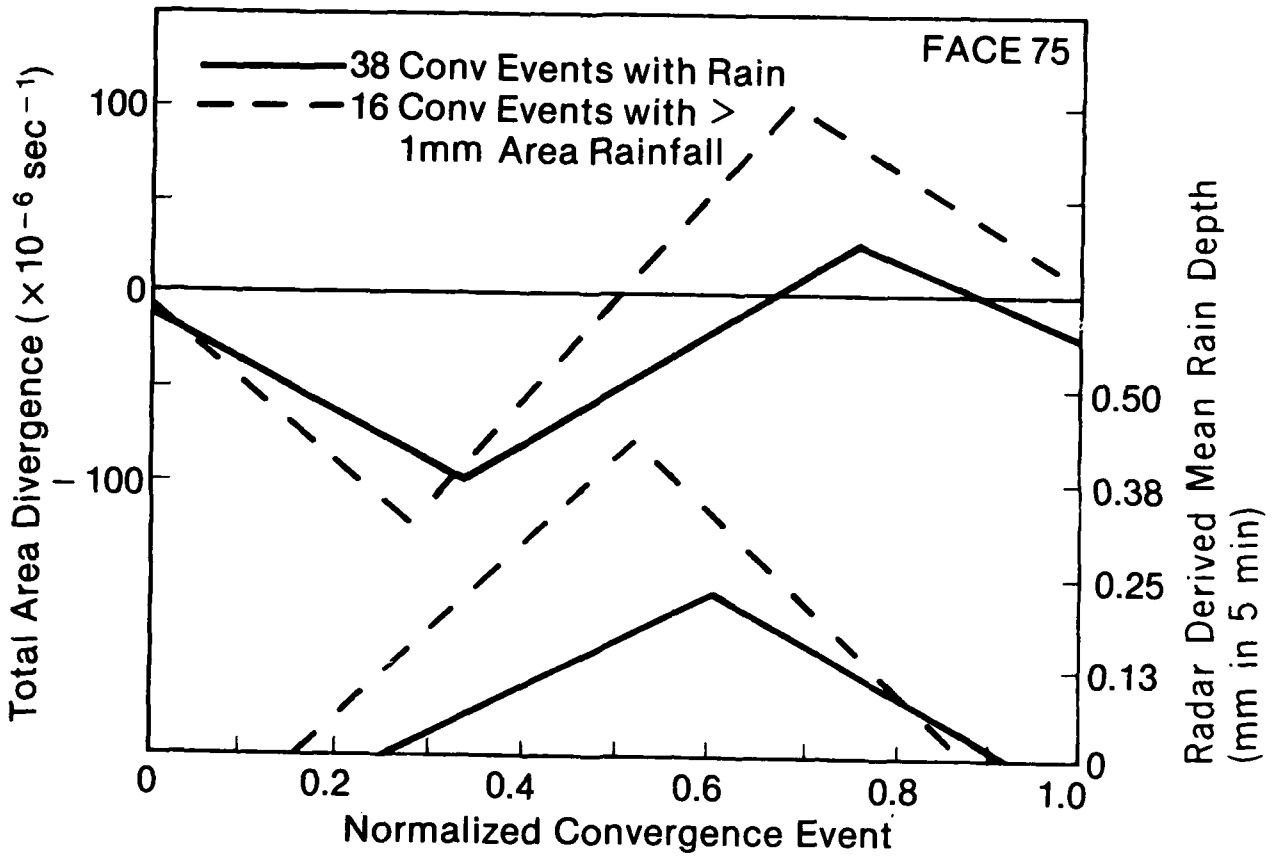

Figure 17. Normalized convergence event for FACE 1975.

Table 3 gives the times between convergence and rain milestones for VIN 1979. Table 10 refers to event milestones for FACE 1975. The most noticeable disagreement is found with the time difference between beginning convergence and initial rain; the time is 35 min for Florida versus 5 min for Illinois. Overall, the times are shorter for Illinois total area divergence, but are respectable for weighted convergence when compared with the south Florida results.

Figs. 18 and 19 show how the convergence-rainfall events fit into 10 and 20 min segments when the difference in time between convergence and rain events given in Tables 3 and 10 are visually depicted. Shaded events account for rain events totaling more than 1 mm. For both FACE and VIN there is a wide spectrum of times, both negative and positive. Negative times exist due to several factors. Precipitation begins with no pulse generated in the area-averaged divergence. The initial triggering mechanism may not be detected by the grid or is too small to be recorded in the averaged field. Difficulties arise separating continuous periods of rain when convergence events occur very close in time (i.e., several hours). In Florida, only 6 events had rain beginning before initial area convergence, but in VIN there are 20 such events; 10 large (> 1mm) events show the problem of moving systems and poor linkage with the boundary layer.

When the time interval is the difference between rain and convergence maxima (middle of Figs. 18 and 19), both FACE and VIN have the mode occurring in the 0- to 20-min interval. Recall from Tables 3 and 10 that the average is 38 min for south Florida and 23 min for Illinois. The time interval between rain maximum and initial convergence (bottom of Figs. 18 and 19) shows an even distribution over a wide range of times; this is indicative of the highly variable nature of the duration and intensity of the convergence and

Table 10. Time in minutes between convergence and rain events based upon August 1975 FACE mesonetwork data.*

	TIME (min)		
	Begin convergence and initial rain	Maximum convergence and rain maximum	Begin convergence and rain maximum
Total Area Divergence	35 (35)	38 (35)	84 (44)
Weighted Convergence	39 (31)	32 (34)	89 (51)

*Standard deviations are in parentheses.

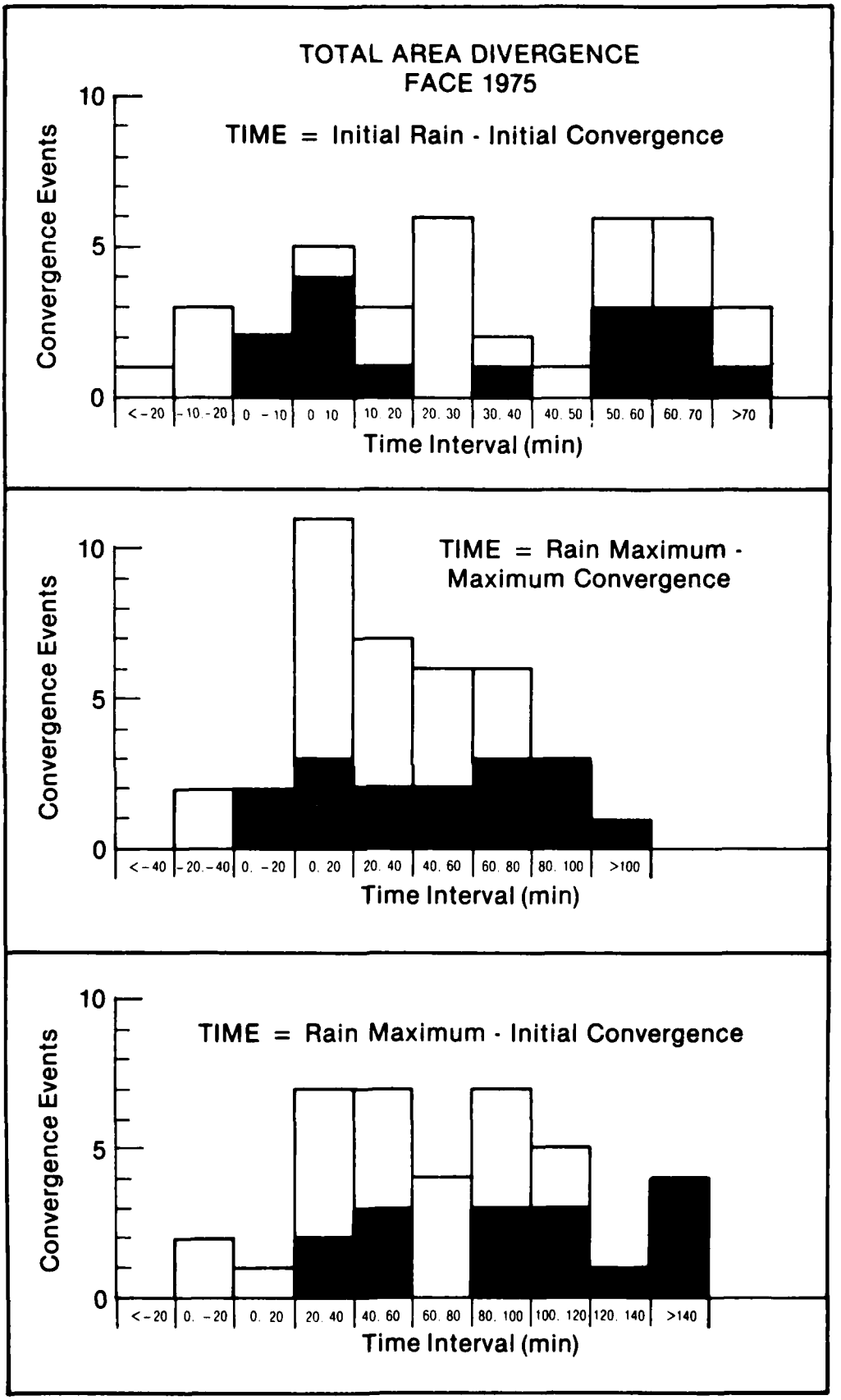

Figure 18. Histogram of the number of convergence events in a particular time interval for FACE 1975. Precipitation events >1 mm are also included.

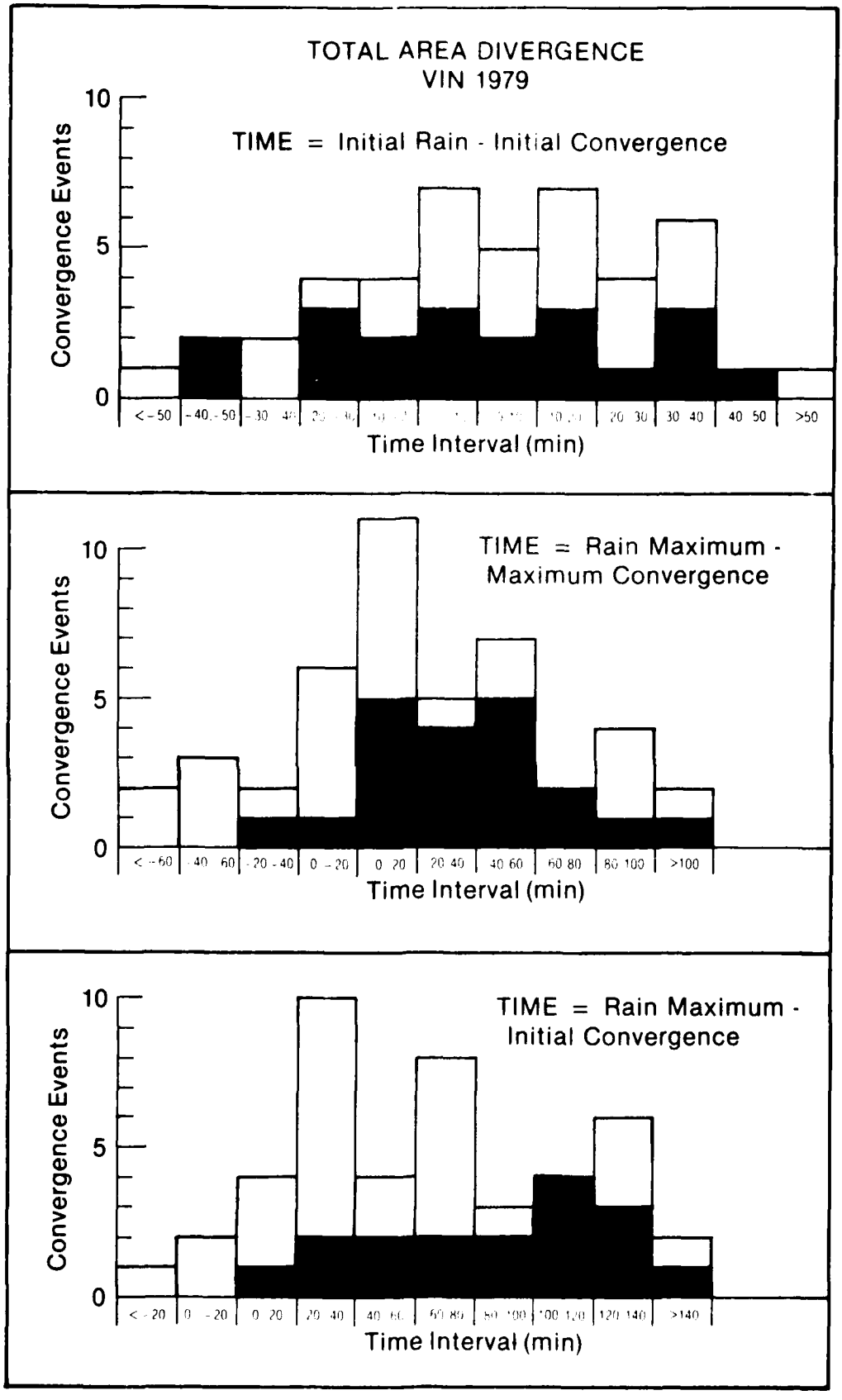

Figure 19. Histogram of the number of convergence events in a particular time interval for VIN 1979. Precipitation events >1 mm are also included.

rainfall. All large rain events (> 1mm) are associated with positive time intervals.

Another question to be asked is how the convergence events are grouped according to the amount of convergence and rainfall. Figs. 20 and 21 examine this question for total area divergence and weighted convergence for FACE 1975 and VIN 1979. Illinois has many more large rain events associated with weak amounts of convergence [(-25 to -50) x 10^{-6} s^{-1}]. Illinois had four large rain events of > 5 mm of area precipitation coupled with weak convergence. FACE had none. A factor that influences the amount of convergence is network size. The VIN network was approximately twice as large as the FACE mesonetwork, which reduces the magnitude of convergence across the larger network.

Total area divergence for VIN finds 56 convergence events in the interval of (-25 to -50) x 10^{-6} s^{-1} that were false alarms (no rain). This interval can hardly be removed since a majority of the precipitation occurred in the interval. Illinois weighted convergence did a much better job by filtering out weaker convergence and rain events.

Subdividing the convergence-rainfall ensemble according to the other forecast parameters is important also. Figs. 22-25 depict how the events group according to middle-level moisture. FACE 1975 data were subdivided into two categories, RH > 52% and RH < 52%, whereas the Illinois ensemble was divided into three categories. In all instances, when middle-level moisture is available, more precipitation occurs. This is seen quite vividly in the VIN data. When middle-level RH < 50%, only two rain events occur with total area divergence and one with weighted convergence.

The question of forecastability of convective rainfall with total area divergence between Florida and Illinois is explored in Fig. 26. Five-minute

values of total area divergence are related to 5-min rainfall at certain time periods (lag) in the future, present, and past. For example, a lag at 25 min relates total area divergence to rainfall that occurs 25 min later. Total area divergence should reflect an inverse correlation between divergence and future rain, and a direct correlation between outflow and precipitation.

Since total area divergence is the sum of weighted convergence and divergence, these two quantities will have one peak each reflecting inflow or outflow. Fig. 26 has been developed using 5-min total area divergence and rainfall from all convergence events found in the Florida and Illinois data. VIN is represented by the solid line and FACE, the dotted line. Comparing Florida and Illinois, the lag versus correlation plots greatly resemble each other. For total area divergence (Fig. 26a), the peak and minimum are within 5 min. Outflow (negative lag) drops a tenth from Florida to Illinois but during inflow (positive lag), total area divergence values in Illinois are slightly better correlated with precipitation (at + 60 min) than in Florida. For weighted convergence (Fig. 26b), the peaks are at 45 min for Florida and 35 min for Illinois, making the lead time between convergence and rainfall greater for Florida. The radar-derived rainfall technique employed in Florida used an observation cone that was approximately 5000 ft (1500 m) over the FACE mesonetwork. This would increase the time lag difference even more if precipitation fall times were considered. In Illinois, weighted convergence increases a tenth in correlation when compared to Florida. The general improvement of weighted convergence was also seen in section 3 because it filtered out weaker insignificant events. Weighted divergence (Fig. 26c) in Illinois is slightly less correlated than Florida. But, weighted divergence, in general, shows the highest correlations yet found between divergence and rainfall.

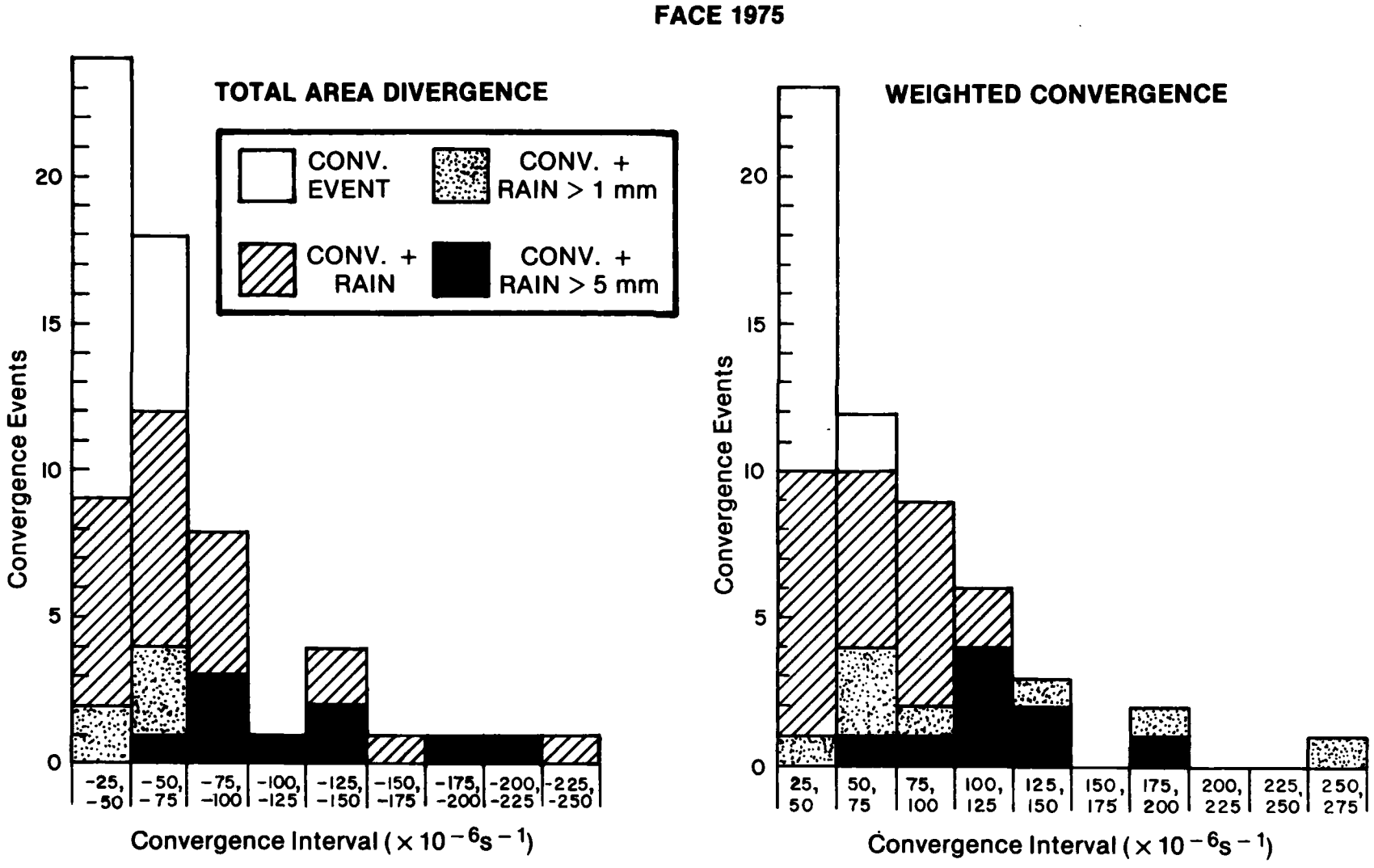

Figure 20. Histograms of the number of convergence events grouped according to the amount of convergence for FACE 1975. Precipitation events are also shown.

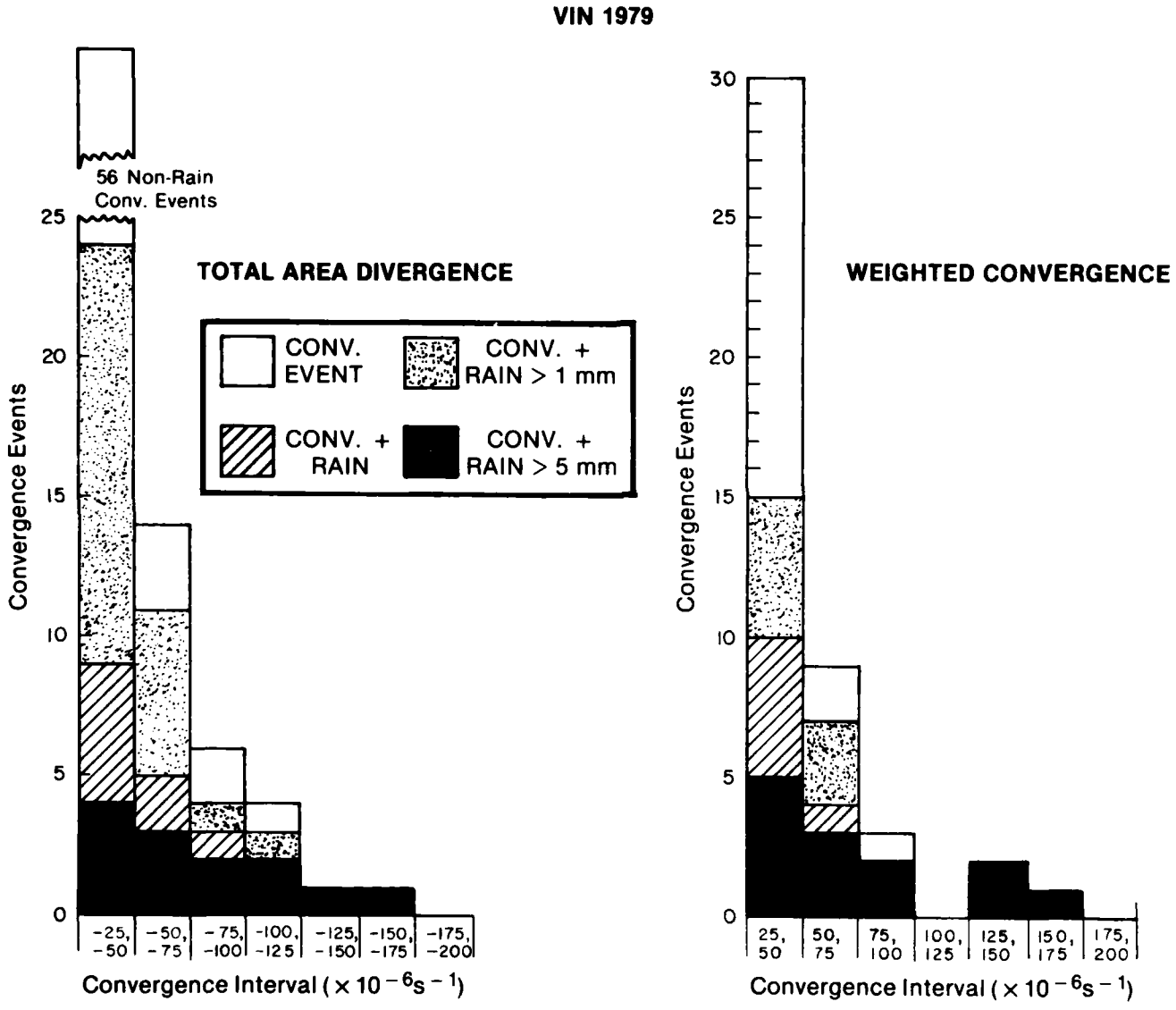

Figure 21. Histograms of the number of convergence events of total area divergence grouped according to the amount of convergence for VIN 1979. Precipitation events are also shown.

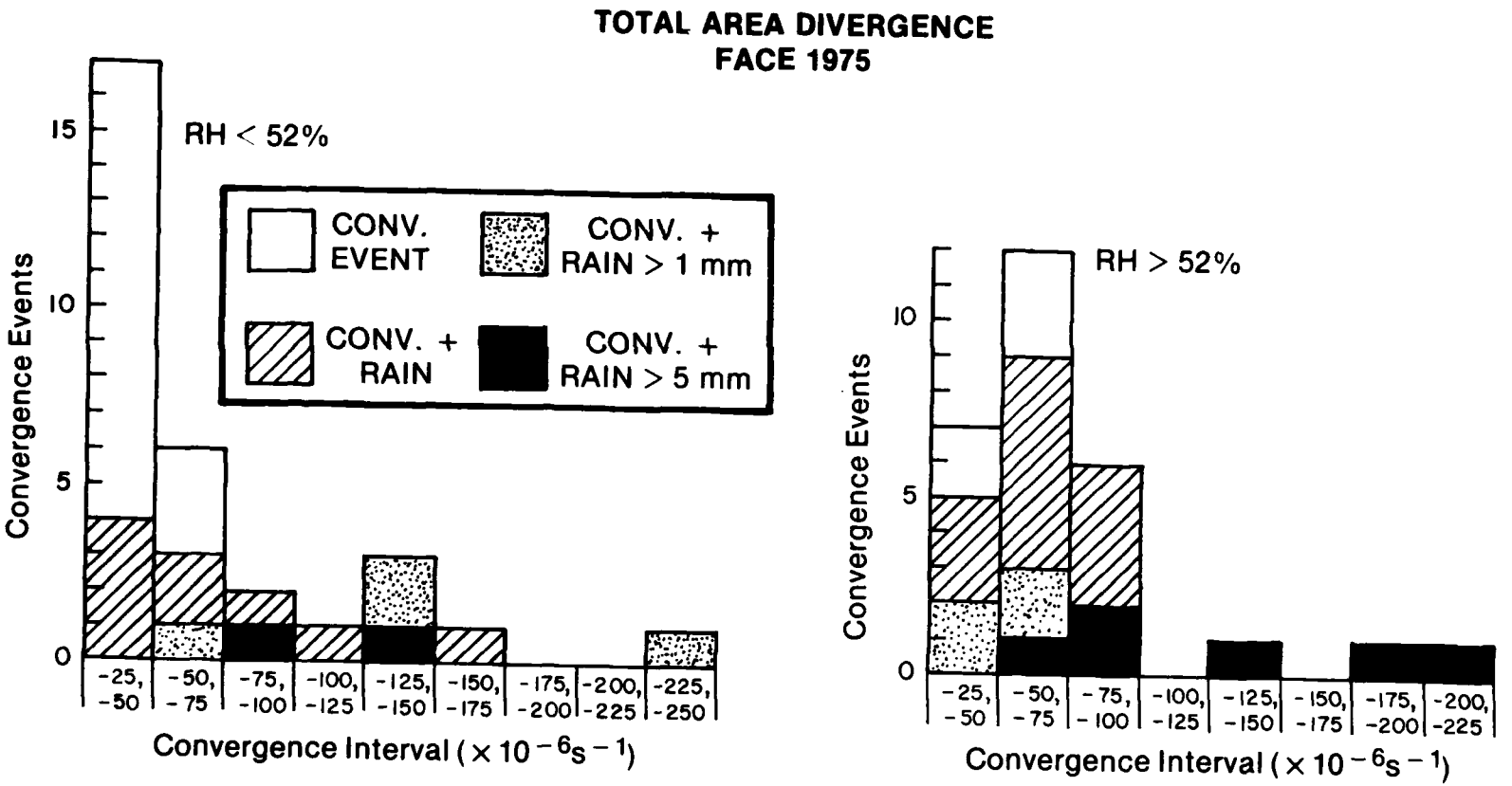

Figure 22. Histograms of the number of convergence events grouped according to the amount of convergence and further subdivided by middle-level moisture for FACE 1975.

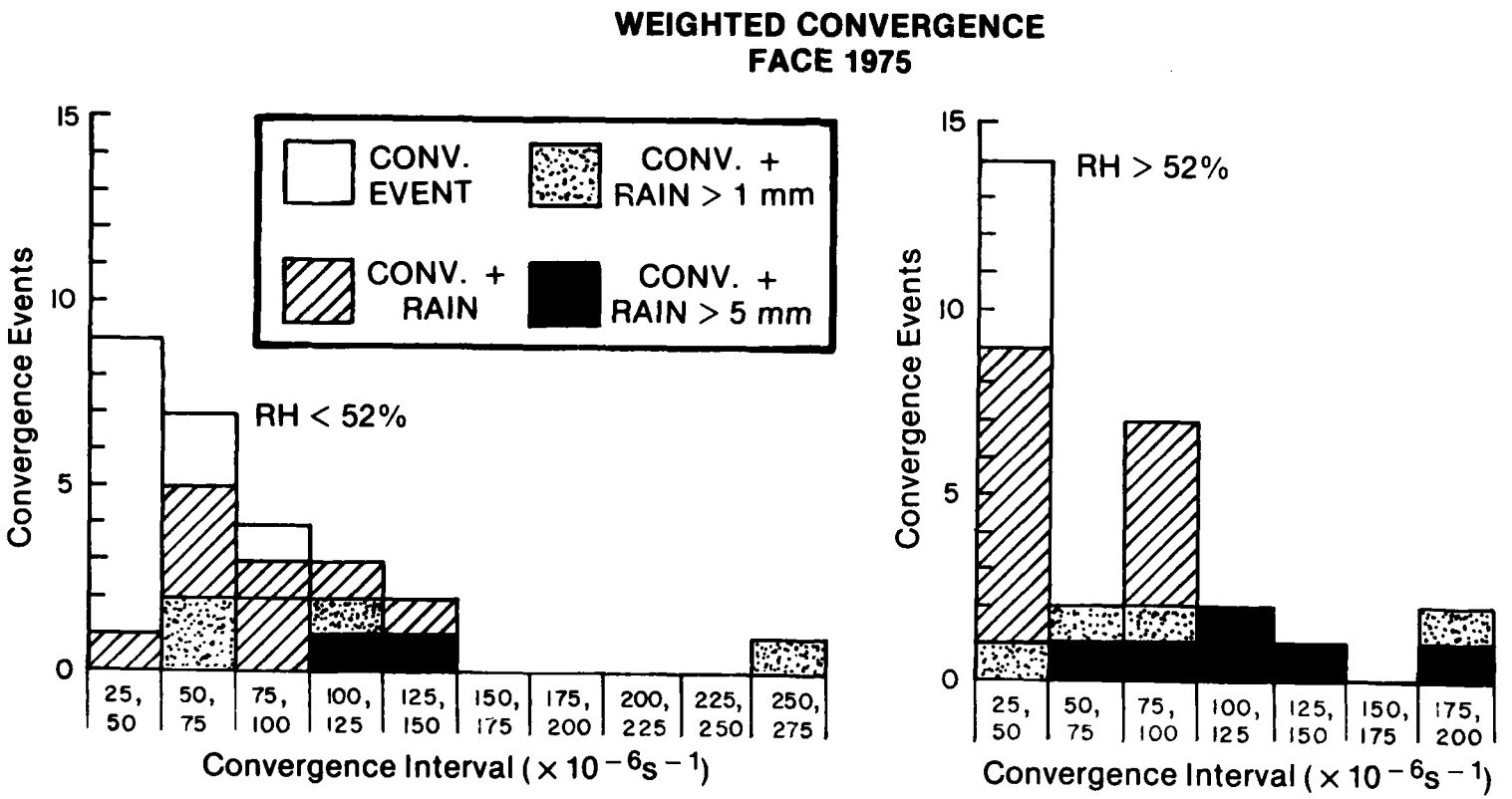

Figure 23. Histograms of the number of convergence events of weighted convergence grouped according to the amount of convergence and further subdivided by middle-level moisture for FACE 1975.

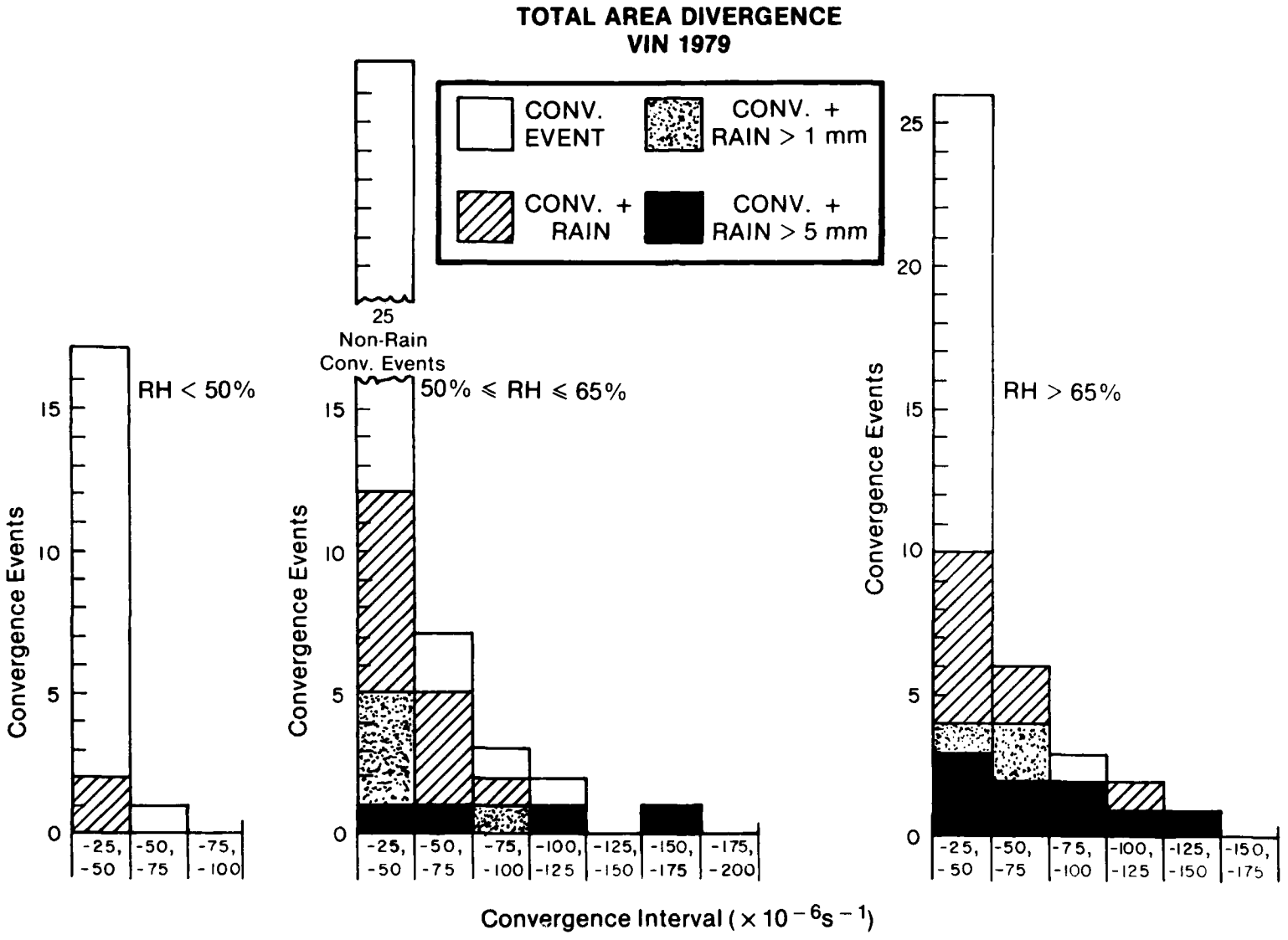

Figure 24. Histograms of the number of convergence events of total area divergence grouped according to the amount of convergence and further subdivided by middle-level moisture for VIN 1979.

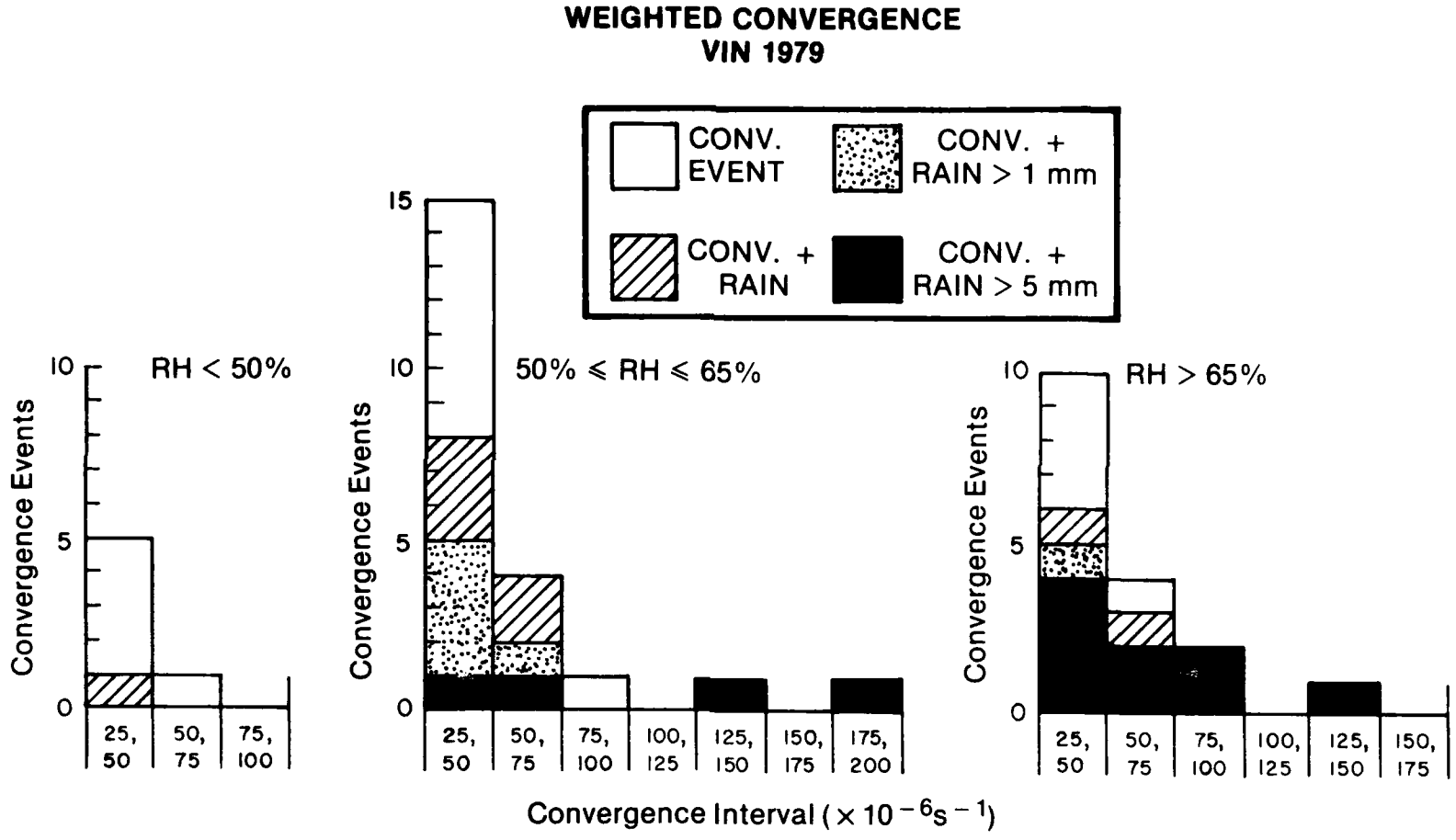

Figure 25. Histograms of the number of convergence events of weighted convergence grouped according to the amount of convergence and further subdivided by middle-level moisture for VIN 1979.

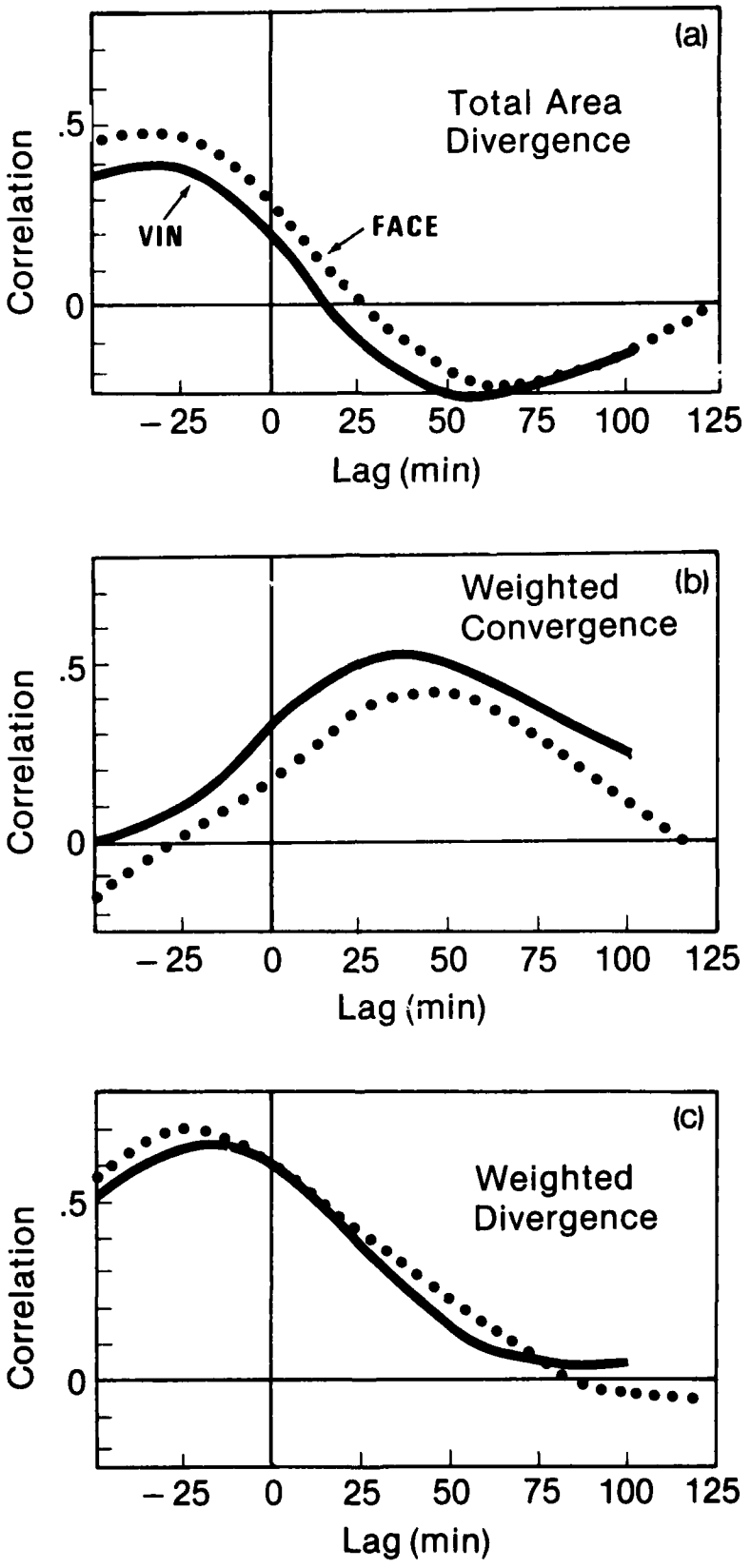

Figure 26. Lag in time between 5-min rain depth and (a) total area divergence, (b) weighted convergence, or (c) weighted divergence versus correlation coefficients of the same parameters -- for FACE and VIN. The dotted line represents FACE; the solid line, VIN.

6. Summary and Conclusions

The problem of nowcasting convective precipitation has been addressed in this report. Two totally different environments have been examined with the same technique. Watson and Blanchard (1982) and Watson et al. (1981) have shown that this method could work in the relatively uncomplicated atmosphere of south Florida. The effect of the network size, sensor separation, and the location and size of the convective activity are critical factors for this scheme to work. Watson et al. (1981) have addressed the questions of the optimum size of the mesoscale region and the effect of station spacing. For area divergence to be of importance, the region must be of a size equal to or somewhat larger than the convective entity being examined. The convective system is fueled from the area surrounding itself and total area divergence is used to measure this process. If the area is too large, a larger spatial scale would be measured and much of the smaller convective activity would be lost. It was found in south Florida that grid separations up to 19.2 km were sufficient to detect reasonable values of total area divergence. The convergence signals from the significant events are enough to be detected by the larger grid spacing.

It was established in south Florida that other meteorological factors play important roles, that is, divergence cannot stand alone. In Florida, these factors included such parameters as low-level wind speed and middle-level moisture. Stability appeared to play an insignificant part. However, stability and moisture were equally important in Illinois. When stability was low, larger amounts of convective rainfall were recorded.

The relative rain output associated with low-level winds showed a reversal from Florida to Illinois. Under weak wind speeds, the Midwest regime yielded less precipitation than under stronger wind speeds. It is natural to

assume that airmass thunderstorms closer to the axis or center of the ridge will produce less precipitation than organized squall lines or frontal activity associated with stronger winds aloft. On the average, 4 ½ times more precipitation occurred with low-level wind speeds > 5 m s^{-1}. In south Florida convection, during times of slow moving convective systems or weak low-level winds, there was 3 times the amount of rainfall per event with just a slight increase in convergence when compared to faster moving systems.

In Illinois, middle-level moisture played its usual role. Under dry conditions (RH < 50%), little or no rain could be expected. But under very moist conditions (RH $\geq$ 65%), heavy precipitation events occur with very little convergence. When the atmosphere has moisture available, it takes a very small amount of energy to start convection going.

Weighted convergence, a subset of total area divergence, was also used to develop regression relationships. Weighted convergence filters out any positive divergence and examines only convergence in the mesonetwork. During the 33 study days, 82% of the total rainfall that occurred was reflected in some manner in weighted convergence. Weighted convergence in Illinois appeared to filter out weak convergence events, therefore eliminating many no-rain or false-alarm convergence events as well as the weaker, unimportant rainfall events. This was not the case in south Florida. This anomaly may be a function of the Illinois data set only and should be examined with other data sets.

The Illinois results have not been all favorable as pictured so far. Correlation coefficients between convergence and rainfall dropped a tenth in nearly all instances when compared with the south Florida results. This shows that convergence aloft becomes even more instrumental in the Midwest. The

surface wind field has less information about the convective inflow patterns than in the more subtropical climate.

The VIN 1979 pibal triangle data were studied in an effort to shed more light on the representativeness of the boundary-layer divergence to surface divergence. The correlation of boundary-layer divergence with surface divergence was discovered to be marginal. Under disturbed meteorological conditions such as convective inflow and outflow, persistent organization of divergence aloft was always found. The sample size of the VIN pibal data was small but the use of boundary-layer divergence as an indicator of convective precipitation was shown. In the future, more efficient wind profiling systems can be used operationally to determine wind convergence and/or moisture flux within the boundary layer, which in turn can be used to make short-term predictions of rainfall. Such remote-sensing devices include clear air Doppler radar profilers and optical systems, all of which are already available.

One of the underlying difficulties with this surface total area divergence technique is that small episodes of area convergence may produce either heavy or light precipitation totals. In south Florida, the larger convergence events always produced moderate to heavy rain events. In Illinois, this was usually the case but several times the pattern was changed by dry outflows accompanied by large convergence originating from convective systems 100 to 200 km from the VIN network. In south Florida, the stronger convective systems were slow moving. In many instances it was possible to record the complete life cycle of the convection within the limits of the FACE mesonetwork. In Illinois, the systems are organized into lines or complexes traversing the VIN mesonetwork in a relatively short time. This manifested

itself in the time between beginning convergence and initial rain, which was 5 min for Illinois and 35 min for south Florida.

The statistical method developed in this study for south Florida and Illinois could be applied to forecast areas of about 3000 km^2 and smaller. Only wind stations surrounding a forecast area are required. With the line integral, there is no need for interior sites. This technique could be done on a daily basis. A threshold for significant precipitation would be predetermined by the user. On the basis of synoptic-scale surface and upper-air reports in the vicinity, and climatology of the local area, a forecast could be made every 12 hours thus informing the user of the possibility for significant precipitation. The user at that time is made aware that the conditions were favorable and significant rain events could occur. The nowcast of predicted amounts of precipitation would be given on the basis of the development of total area divergence in the area under consideration with lead times of 30 to 60 min. Application of this technique could include the forecasting of precipitation for a metropolitan area, watershed, or agricultural region.

ACKNOWLEDGMENTS

This research was supported by the Army Research Office, Department of Defense, and the Atmospheric Research Section, National Science Foundation, under NSF Grant ATM-78-08865.

Deep appreciation is extended to Dr. Bernice Ackerman at the Illinois State Water Survey for her leadership role in the VIN project. Many thanks go to Margie Casey, Jeff Morris, Jim Hansen, Gerardo Garcia, Randal Carrol and Ed Good, who did various aspects of VIN data reduction.

Gratitude is also extended to the personnel of the Illinois State Water Survey and the University of Virginia who coordinated and participated in the VIN field project of 1979.

References

Ackerman, B., R. W. Scott, and N. E. Westcott, 1982: Summary of field operations and observations, Summer 1979. Tech. Rept. No. 1, Illinois State Water Survey, Champaign-Urbana, Ill.

Arya, S. P. S., and J. C. Wyngaard, 1975: Effect of baroclinicity on wind profiles and the geostrophic drag law for the convective planetary boundary layer. J. Atmos. Sci. 32:767-778.

Brock, F. V., and P. K. Govind, 1977: Portable Automated Mesonet in operation. J. Appl. Meteor. 16:299-310.

Brown, J. M., and A. R. Hansen, 1978: Water budget of cumulonimbus clusters and of the peninsula scale over south Florida. Final report, Grant No. 04-7-022-4430 from National Hurricane and Experimental Meteorology Laboratory to Iowa State Univ., NOAA Environmental Research Laboratories, Boulder, CO., 220 pp.

Byers, H. R., and R. R. Braham, Jr., 1949: The Thunderstorm, U. S. Gov. Printing Office, Washington, D.C., 287 pp.

Byers, H. R., and E. C. Hull, 1949: Inflow patterns of thunderstorms as shown by winds aloft. Bull. Amer. Meteor. Soc. 30:90-96.

Changnon, S. A., and F. A. Huff, 1980: Review of Illinois Summer Precipitation Conditions. Illinois State Water Survey Bulletin 64, 160 pp.

Cooper, H. J., M. Garstang, and J. Simpson, 1982: The diurnal interaction between convection and peninsular scale forcing over south Florida. Submitted to Mon. Wea. Rev.

Cressman, G. P., 1959: An operational objective analysis system. Mon. Wea. Rev. 87:367-374.

Goff, R. C., 1975: Thunderstorm - outflow kinematics and dynamics. NOAA Tech. Memo. ERL NSSL-75, Norman OK, 63 pp.

Lhermitte, R. M., and M. Gilet, 1975: Dual-Doppler radar observation and study of a sea breeze convective storm development. J. Appl. Meteor. 14:1346-1361.

Ulanski, S. L., and M. Garstang, 1978: The role of surface divergence and vorticity in the life cycle of convective rainfall. Part I: Observations and analysis. J. Atmos. Sci. 35:1047-1062.

Watson, A. I., and D. O. Blanchard, 1982: The relationship between low-level convergence and convective precipitation in south Florida. Submitted to Mon. Wea. Rev.

Watson, A. I., R. L. Holle, J. B. Cunning, P. T. Gannon and D. O. Blanchard, 1981: Low-level convergence and the prediction of convective precipitation in south Florida. Tech. Rept. No. 4, NOAA Environmental Research Laboratories, Office of Weather Research and Modification, Boulder, Colo. and Illinois State Water Survey, Champaign-Urbana, Ill. (National Technical Information Service, Springfield, VA., AD-A097 553/2), 228 pp.

END

FILMED

6-83

DTIC